Flux Vector Distribution

Robert Struijs *

6 january 2010

Abstract. We present a space discretization for advection equations on unstructured and structured grids. In this discretization, the flux is calculated on edges, and then distributed over the nodes of the grid. The distribution is based on advection speeds which are edge-based or cell-based, corresponding to flux vector splitting or to flux difference splitting. Enlarging the distribution stencil leads to upwind and central directional higher order schemes. The discretization method includes and extends residual distribution methods. In this paper, the distribution is based on the N scheme since the aim is to reduce the truncation error for certain directions, but the method allows for more general distributions with improved accuracy. For systems of equations, the flux vector is decomposed in scalar parts which are distributed separately. Discretizations using limiters are locally inconsistent.

Key words : Distribution schemes, flux splitting, N scheme, limiter, consistency.

AMS subject classification : 65M06.

1. Introduction.

The Finite Volume (FV) method is frequently used for the discretization of advection equations. The FV method is closely linked to the integral form of the partial differential equations, and leads easily to a scheme in conservation form. Its geometrical flexibility contributes to its popularity. In the FV method, the volume-centered unknowns represent the volume-averaged state. They are used to approximate the interface fluxes through the edges in a central or upwind manner. The contour integral of the flux is then used to advance the unknowns to the next time level. More accurate schemes are obtained with higher order interpolation of variables or fluxes. Limiters or artificial viscosity lead to monotone solutions.

Godunov's method [1] of solving the Riemann problem has inspired approximate upwind solvers which use for the upwind flux calculation Flux Difference Splitting (FDS). In the FDS method, the flux difference between two neighboring states is decomposed in waves related to the local Riemann problem [2, 3]. The waves arriving at the edge are added to approximate the interface flux [4, 5].

In the Flux Vector Splitting (FVS) upwind method, the flux in a cell is split in parts depending on the velocities in the cell. The interface flux is the sum of those parts which have velocities toward the interface. There is a close relationship with Boltzmann schemes, where particles move in and out of a cell with a certain velocity distribution [6, 7].

In two or three dimensions, the approximation of the numerical flux at a cell boundary is essentially a grid related one-dimensional process. Efforts have been made to remove this restriction by upwinding along grid independent directions like streamlines and bi-characteristics in the case of systems of equations, see e.g. [8]–[17], and references therein. Multi-dimensional upwind methods are not yet widely accepted, contrary to grid-normal based methods. In the case of systems of equations with non-commuting Jacobians, early versions had problems of convergence and monotonicity.

A closely related alternative to the FV method is the Residual Distribution (RD) method[1], which has been developed over the past thirty years [18]-[25]. The unknowns are

*Dimitsanis 14, 14564 N. Kifissia, Greece ; robert.struijs@free.fr.

[1]Also called : residual splitting or fluctuation splitting.

placed at the nodes of the grid, using a Finite Element (FE) type of representation. The residual is calculated on a volume of the structured or unstructured mesh. An approximation is involved in distributing the residuals to the nodes. Scalar distribution discretizations have been formulated for triangular grids [21]-[26]. Certain properties can be imposed such as monotonicity preservation and linearity preservation. The latter corresponds to second order accuracy on structured grids. Among the distribution discretizations are the Lax-Wendroff scheme (linearity preserving, not monotone), the upwind N-discretization (N for narrow, first order, monotone), the PSI discretization, which is a minmod limited N-discretization, and the LDA discretization (linearity preserving, not monotone). The residual distribution formulation works fine for the scalar advection equation, and shows advantages over the standard finite volume upwind discretizations. For systems of equations, first upwind attempts with the RD method were with the wave models of Roe [27, 26], which is a multi-dimensional extension of the one-dimensional FDS of Roe. This was followed by a hybrid method [28], solving the acoustic part with the Lax-Wendroff scheme. Matrix distribution schemes [29] have been cast into the RD framework [30, 31]. Several publications report extensions to higher order discretizations [32, 33, 34]. Changing the linear variation of the unknowns to a higher order variation presents complications with the linearization for systems of equations.

We present in this paper a flux distribution method. Contrary to the RD method where the fluxes are gathered into a residual, which is distributed using a cell-averaged speed, the individual flux at an edge of the grid will be distributed over the nodes. The distribution depends on the local advection speed at the edge, or on the advection speeds of the adjacent cells, and corresponds to FVS or FDS.

This paper is organized as follows. First, discretizations in one dimension are cast in a FVD formulation, assuming linearly varying unknowns. In one dimension, edges and sides collapse to nodes. Therefore, the flux is calculated at the nodes and distributed based on a node-based or cell-based advection speed. Classical discretizations are recovered with an appropriate choice of the distribution of the flux. Higher order discretizations with nonlinear variation of the unknowns are possible, but are not exploited in this paper. Instead, we consider distributions to more distant nodes. The FVS or FDS extension to systems of equations makes use of a flux splitting in scalar parts or waves, with corresponding advection speeds.

In the following section, discretizations for two space dimensions are treated. The RD formulation of the N scheme on a triangle is the starting point for the derivation of the FVD N scheme. The N scheme is an example of a directional discretization, i.e. a discretization which aims to reduce specific terms in the truncation error given a preferential direction. Distribution to more distant nodes leads to the second order N scheme. The discretizations are analyzed for accuracy and consistency. Using a structured grid of triangles, a second order directional upwind discretization for structured meshes is derived.

It appears that discretizations with a distribution derived from the N scheme can be inconsistent on unstructured grids. This is the case in two dimensions when a node is not surrounded by six triangles. In three dimensions, inconsistency appears for the icosahedron and for structured grids where the cubes are dissected in tetrahedra.

The N scheme is not an essential part of the FVD method. More general discretizations which can be rewritten in the FVD formulation, some of which with better accuracy or stability, are described in a separate paper [35].

2. One-dimensional schemes in the Flux Vector Distribution formulation.

We start with discretizations of the scalar advection equation in nonlinear or linear form,

$$\frac{\partial u}{\partial t} + \frac{\partial f}{\partial x} = 0\,, \quad \text{or} \quad \frac{\partial u}{\partial t} + a\frac{\partial u}{\partial x} = 0\,, \quad \text{with} \quad a = \frac{\partial f}{\partial u}\,, \tag{2.1}$$

on a regular grid with nodes $x = x_i$ and grid spacing Δx. We will restrict the analysis to explicit schemes. We recapitulate the Finite Volume (FV) and Residual Distribution (RD) methods for a clearer presentation and better comprehension of the Flux Vector Distribution (FVD) formulation.

2.1. Three point schemes.

Consider the space discretizations on the three point stencil $i-1, i, i+1$. The upwind schemes on this stencil will be first order, the central scheme second order.

2.1.1. The Finite Volume scheme.

The volume for node i in the FV method is $[x_{i-1/2}, x_{i+1/2}]$. Over this volume, the unknowns u_i are assumed constant. The numerical flux $f_{i\pm1/2}$ is approximated at $x_{i\pm1/2}$ using u_i and the neighboring values $u_{i\pm1}$. The cell residual R_i is the difference of the approximated numerical fluxes $f_{i+1/2} - f_{i-1/2}$. With forward Euler time stepping, this leads to the standard update

$$u_i^{n+1} - u_i^n = -\frac{\Delta t}{\Delta x}\, R_i = -\frac{\Delta t}{\Delta x}\, \left\{ f_{i+1/2} - f_{i-1/2} \right\}\,. \tag{2.2}$$

The scheme is indicated in Fig. 2.1, where the dotted arrows indicate the computation of the interface fluxes, *approximated* from the nodal values, and the solid arrows show the construction of the residual from the fluxes and the update from the residual.

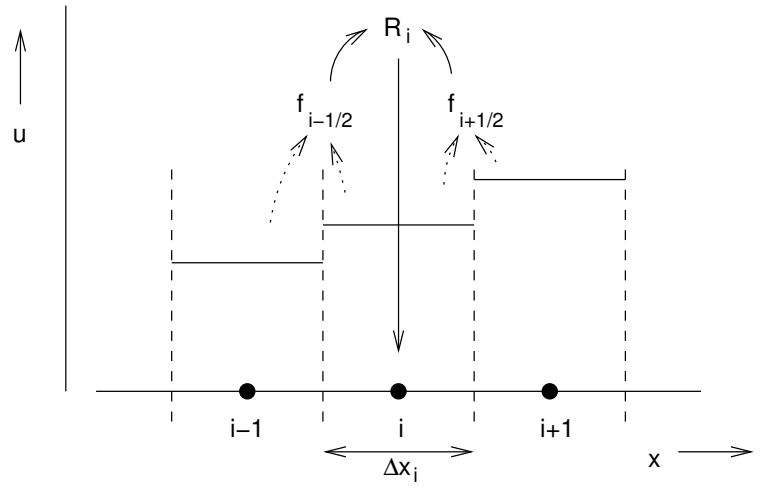

Figure 2.1. Discretization of (2.1) with the FV scheme, approximating the fluxes $f_{i\pm1/2}$ for the computation of the residual R_i which is used in the update of node u_i.

Well-known schemes are the central scheme, $f_{i+1/2} = {}^1\!/_2\, \{f_i + f_{i+1}\}$, and the upwind schemes. Upwind schemes are classified as FVS and FDS, and come in a great variety, see e.g. [2, 3]. The main difference between the schemes is in the way they capture discontinuities of the solution.

The interface flux for FVS can be written as $f_{i+1/2} = f_i^+ + f_{i+1}^-$. The update for node i becomes

$$u_i^{n+1} - u_i^n = -\frac{\Delta t}{\Delta x} \left\{ f_i^+ - f_{i-1}^+ + f_{i+1}^- - f_i^- \right\} . \tag{2.3}$$

An example of a FDS flux is

$$f_{i+1/2} = \tfrac{1}{2} \left\{ f_i + f_{i+1} \right\} - \tfrac{1}{2} \left| a_{i+1/2} \right| \left(u_{i+1} - u_i \right) , \tag{2.4}$$

where the cell-wise speed $a_{i+1/2}$ satisfies

$$f_{i+1} - f_i = a_{i+1/2} \left(u_{i+1} - u_i \right) , \tag{2.5}$$

and the update for node i is obtained with (2.2). For the linear advection equation with $a > 0$, the upwind schemes revert to $f_{i+1/2} = f_i$ and $u_i^{n+1} - u_i^n = -(\Delta t/\Delta x) \left(f_{i+1} - f_i \right)$.

2.1.2. The Residual Distribution scheme.

In the RD method [18, 19, 22], the solution is approximated by a continuous piece-wise linear function often used in FE methods,

$$u(x,t) = \sum_i u_i(t)\, w_i(x) , \tag{2.6}$$

where $w_i(x)$ is the piece-wise linear basis function. With this representation, the space integral of the time derivative of (2.1) becomes $\int_{x_1}^{x_N} (\partial u_i/\partial t)\, \mathrm{d}x = \sum_{i=1}^{N} l_i \, (\partial u_i/\partial t)\, \mathrm{d}x$. The nodal volumes are the intervals $l_i = x_{i+1/2} - x_{i-1/2} = 1/2 \, (x_{i+1} - x_{i-1})$, $l_1 = 1/2 \, (x_2 - x_1)$, and $l_N = 1/2 \, (x_N - x_{N-1})$. The residual computed on the interval $(i, i+1)$, $R_{i+1/2} = \int_{x_i}^{x_{1+1}} (\partial f/\partial x)\, \mathrm{d}x = f_{i+1} - f_i$, is distributed over the nodes $i+1$ and i such that $\delta u_i := \delta u_i - (\Delta t/l_i)\, \alpha_i^{i+1/2} R_{i+1/2}$, and $\delta u_{i+1} := \delta u_{i+1} - (\Delta t/l_{i+1})\, \alpha_{i+1}^{i+1/2} R_{i+1/2}$. In the notation of the distribution coefficient α_n^c, c indicates the cell where the residual is calculated, while n is the node to which it is sent. The scheme is shown in Fig. 2.2, where the solid arrows indicate the computation of the flux from the nodal values, the construction of the residual from the nodal fluxes, and the dotted arrows the *approximated* update from the distribution of the residual.

The update for node i on a three point stencil can then be written as a sum of contributions from the neighboring residuals,

$$u_i^{n+1} = u_i^n - \frac{\Delta t}{l_i} \sum_{j=i-1/2}^{i+1/2} \alpha_i^j R_j \, . \tag{2.7}$$

The weights $\alpha_i^{i+1/2}$ and $\alpha_{i+1}^{i+1/2}$ determine the properties of the scheme. Distribution of the entire residual of each cell, i.e. $\alpha_{i+1}^{i+1/2} + \alpha_i^{i+1/2} = 1$, ensures conservation [21]. Note that in [21] the fluctuation $\phi_{i+1/2} = -R_{i+1/2}$ is distributed.

The central scheme is obtained by equidistribution of the residual $R_{i+1/2}$ over nodes i and $i+1$ with $\alpha_{i+1}^{i+1/2} = \alpha_i^{i+1/2} = 1/2$. For some upwind schemes the same linearized advection speed $a_{i+1/2}$ is used as in the FV method with the Roe solver. For $a_{i+1/2} > 0$, $\alpha_{i+1}^{i+1/2} = 1$ and $\alpha_i^{i+1/2} = 0$, and $R_{i+1/2}$ is subtracted from the update of node $i+1$; if $a_{i+1/2} < 0$, $\alpha_{i+1}^{i+1/2} = 0$ and $\alpha_i^{i+1/2} = 1$, and node i receives $-R_{i+1/2}$. The distribution coefficients can be written in short as $\alpha_{i+1}^{i+1/2} = 1/2 \, (1 + \mathrm{sgn}(a_{i+1/2}))$ and $\alpha_i^{i+1/2} = 1 - \alpha_{i+1}^{i+1/2} =$

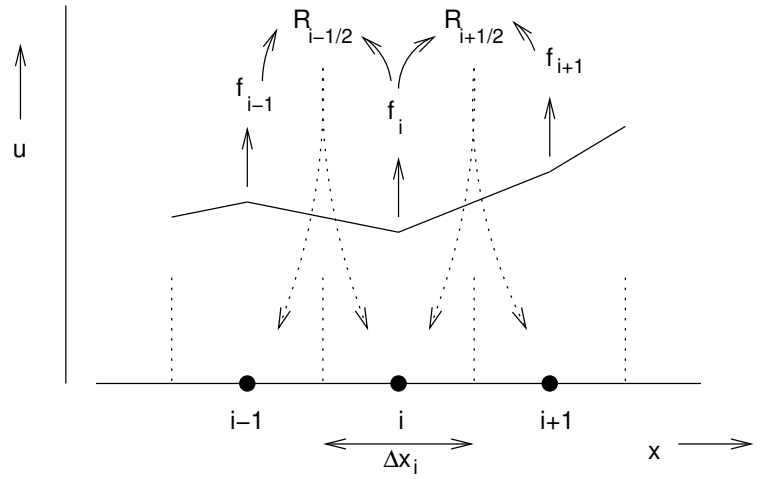

Figure 2.2. Discretization of (2.1) with the RD scheme, computing the residual R_i with nodal fluxes, and approximately updating the node u_i with parts of the residuals.

$1/2\,(1-\mathrm{sgn}(a_{i+1/2}))$. With these coefficients we can write $\alpha_i^{i-1/2} R_{i-1/2} = 1/2\,\{f_i - f_{i-1}\} + 1/2\,|a_{i-1/2}|\,(u_i - u_{i-1})$ and $\alpha_i^{i+1/2} R_{i+1/2} = 1/2\,\{f_{i+1} - f_i\} - 1/2\,|a_{i+1/2}|\,(u_{i+1} - u_i)$. The resulting update for node i is identical to (2.2) and (2.4). The method is in one dimension just an alternative to the FDS method of the FV discretization, §2.1.1. In two and three dimensions, however, the distribution coefficients can be tuned to the advection speed. This reduces the grid dependence of the schemes and increases the accuracy and stability.

2.1.3. The Flux Vector Distribution scheme.

The solution is approximated by a continuous piece-wise linear function like in the RD method, (2.6). But instead of assembling the fluxes into a residual which is distributed with an averaged advection speed, the fluxes are distributed individually according to the local advection speed $a_i = \left.\frac{\partial f}{\partial u}\right|_i$, or the adjacent cell advection speeds $a_{i-1/2}$ and $a_{i+1/2}$. This enables the formulation of both the FVS and the FDS schemes mentioned in the FV discretization, §2.1.1. The scheme is indicated in Fig. 2.3, where the solid arrows indicate the computation of the flux from the nodal values, and the dotted arrows the *approximated* update from the distribution of the nodal fluxes.

Let the effect of flux f_i at node j be given by $\delta u_j := \delta u_j - (\Delta t/l_j)\,\alpha_j^i f_i$. The distribution coefficients α_n^e determine the properties of the scheme, where e stands for the edge interface (node in one dimension, surface in three dimensions) where the flux is calculated, and n the receiving node. We maintain the sign convention of the RD method. It has the advantage that the distribution coefficients are just the coefficients appearing in a standard finite difference expression of the residual. For conservation we need $\sum_j \alpha_j^i = 0\ \forall\, i$ except for $i = 1$ or $i = N$ at the boundaries of the domain. The update for node i on a three point stencil can then be written as

$$u_i^{n+1} = u_i^n - \frac{\Delta t}{l_i} \sum_{j=i-1}^{i+1} \alpha_i^j f_j\,. \tag{2.8}$$

Upwind schemes. We use the standard notation

$$a^{\pm} = \tfrac{1}{2}(a \pm |a|)\,, \quad \text{with} \quad a^+ \geq 0\,, \quad a^- \leq 0\,, \quad a^+ + a^- = a\,, \quad a^+ - a^- = |a|\,, \tag{2.9}$$

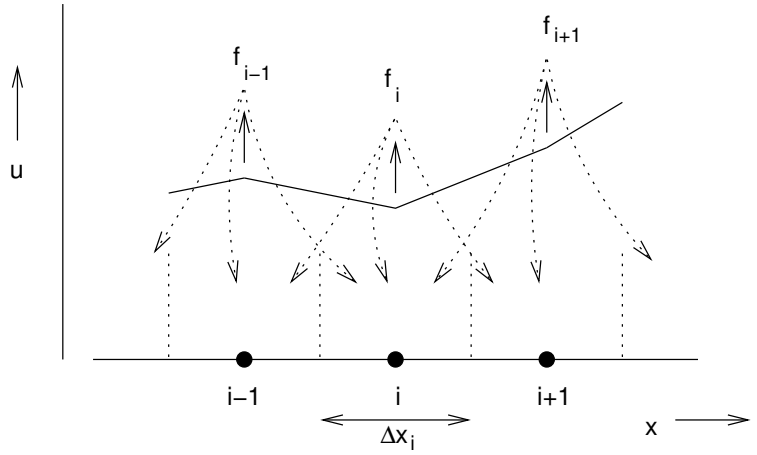

Figure 2.3. Discretization of (2.1) with the FVD scheme, where the approximated update of node u_i involves the nodal fluxes f_{i-1}, f_i, and f_{i+1}.

and for $a \neq 0$ the adimensional directional coefficients d,

$$d = \frac{a}{|a|} = \pm 1 = \mathrm{sgn}(a)\,, \quad d = \frac{1}{d}\,, \quad \text{with} \quad d^{\pm} = \tfrac{1}{2}(d \pm |d|)\,,$$
$$d^{+} \geq 0\,, \quad d^{-} \leq 0\,, \quad d^{+} + d^{-} = d = \pm 1\,, \quad d^{+} - d^{-} = |d| = 1\,. \tag{2.10}$$

Flow-dependent switching functions have been introduced by Murman and Cole [36] for their central-upwind discretization. Switching functions are also found in the flux splitting of Engquist and Osher [37]. The extension of these coefficients to more space dimensions and to systems of equations is trivial.

A normalized flux which has $f = 0$ for $a = 0$ is insensitive to the discontinuity of the coefficient d.

The distribution of the nodal flux can be based on the nodal advection speed $a_i = {}^{\partial f}/_{\partial u}|_i$ or on the cell advection speeds $a_{i-1/2}$ and $a_{i+1/2}$.

With the distribution based on the nodal speed, the distribution coefficients for the flux f_i are

$$\begin{aligned} &\text{for } a_i > 0: \quad \alpha^i_{i-1} = 0\,, \quad \alpha^i_i = 1\,, \quad \alpha^i_{i+1} = -1\,, \\ &\text{for } a_i < 0: \quad \alpha^i_{i-1} = 1\,, \quad \alpha^i_i = -1\,, \ \alpha^i_{i+1} = 0\,, \end{aligned} \tag{2.11}$$

or

$$\alpha^i_{i-1} = -d^-_i\,, \quad \alpha^i_i = d^+_i + d^-_i = d_i\,, \quad \text{and} \quad \alpha^i_{i+1} = -d^+_i\,. \tag{2.12}$$

The distribution for $a_i > 0$ is indicated in Fig. 2.4.

The fluxes which are distributed to the nodes $i-1$, i, and $i+1$ are $\alpha^i_{i-1} f_i = -d^-_i f_i = f^-_i$, $\alpha^i_i f_i = (d^+_i + d^-_i) f_i = d_i f_i = f^+_i - f^-_i = |f_i|$, and $\alpha^i_{i+1} f_i = -d^+_i f_i = -f^+_i$ respectively. The update of node i then becomes

$$\begin{aligned} u^{n+1}_i - u^n_i &= -\frac{\Delta t_i}{\Delta x_i} \left\{ \alpha^{i-1}_i f_{i-1} + \alpha^i_i f_i + \alpha^{i+1}_i f_{i+1} \right\} \\ &= -\frac{\Delta t_i}{\Delta x_i} \left\{ -d^+_{i-1} f_{i-1} + (d^+_i + d^-_i) f_i - d^-_{i+1} f_{i+1} \right\} \end{aligned}$$

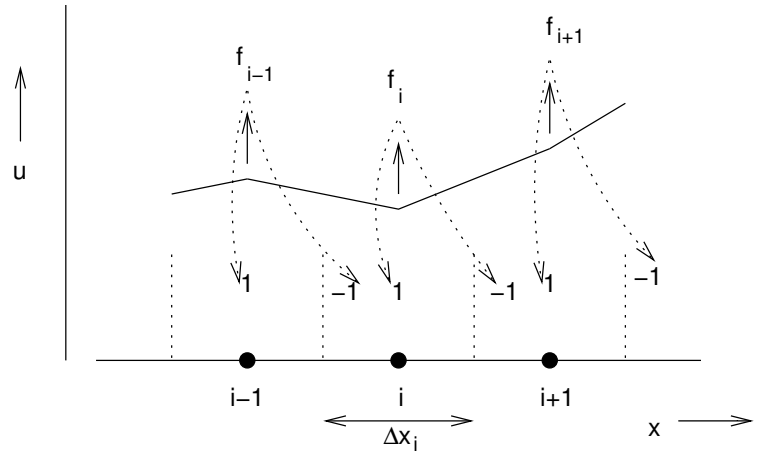

Figure 2.4. Discretization of (2.1) with the FVD scheme for $a_i > 0$: the fluxes are distributed downstream with the weights as indicated.

$$= -\frac{\Delta t_i}{\Delta x_i} \left\{ f^-_{i+1} + f^+_i - (f^-_i + f^+_{i-1}) \right\} . \tag{2.13}$$

This is the FVS scheme of (2.3) derived in a FVD context. The interface fluxes are

$$f_{i+1/2} = d^+_i f_i - d^-_{i+1} f_{i+1} = f^+_i + f^-_{i+1} . \tag{2.14}$$

For the distribution with the cell advection speeds we use the coefficients α based on speed $a_{i-1/2}$ to send the flux f_i to nodes $i-1$ and i, and coefficients β based on speed $a_{i+1/2}$ to send the flux f_i to nodes i and $i+1$, similar to (2.11),

$$\begin{aligned} &\alpha^i_{i-1} = -d^-_{i-1/2} , \quad \alpha^i_i = d^+_{i-1/2} , \quad \alpha^i_{i+1} = 0 , \\ &\beta^i_{i-1} = 0 , \qquad\qquad \beta^i_i = d^-_{i+1/2} , \quad \beta^i_{i+1} = -d^+_{i+1/2} . \end{aligned} \tag{2.15}$$

The update of node i and the interface fluxes using (2.15) is

$$\begin{aligned} u^{n+1}_i - u^n_i &= -\frac{\Delta t_i}{\Delta x_i} \left\{ (\alpha^{i-1}_i + \beta^{i-1}_i) f_{i-1} + (\alpha^i_i + \beta^i_i) f_i + (\alpha^{i+1}_i + \beta^{i+1}_i) f_{i+1} \right\} \\ &= -\frac{\Delta t_i}{\Delta x_i} \left\{ -d^+_{i-1/2} f_{i-1} + (d^+_{i-1/2} + d^-_{i+1/2}) f_i - d^-_{i+1/2} f_{i+1} \right\} \\ &= -\frac{\Delta t}{\Delta x} \left\{ -d^-_{i+1/2} (f_{i+1} - f_i) + d^+_{i-1/2} (f_i - f_{i-1}) \right\} \\ &= -\frac{\Delta t_i}{\Delta x_i} \left\{ \tfrac{1}{2} \{ f_{i+1} - f_{i-1} \} - \tfrac{1}{2} d_{i+1/2} (f_{i+1} - f_i) + \tfrac{1}{2} d_{i-1/2} (f_i - f_{i-1}) \right\} , \end{aligned} \tag{2.16}$$

$$f_{i+1/2} = d^+_{i+1/2} f_i - d^-_{i+1/2} f_{i+1} = \tfrac{1}{2} \{ f_{i+1} + f_i \} - \tfrac{1}{2} d_{i+1/2} (f_{i+1} - f_i) . \tag{2.17}$$

This formulation leaves freedom in the choice of $a_{i-1/2}$ and $a_{i+1/2}$. The trivial choice is to take some average, e.g.

$$a_{i+1/2} = \tfrac{1}{2}(a_i + a_{i+1}) , \quad \text{or} \quad a_{i+1/2} = \left. \frac{\partial f}{\partial u} \right|_{i+1/2} , \tag{2.18}$$

or the advection of (2.5). With the second choice of (2.18) we obtain the flux difference splitting of Huang [38]. For a discussion see [2].

There are still other distributions possible. We can use the distribution of (2.11) with the average of the cell speeds, $\overline{a} = {}^1\!/_2(a_{i-1/2} + a_{i+1/2})$. This gives (2.13) and (2.14) based on $\overline{a}$. The same result is obtained when half of the flux is distributed with each of the cell advection speeds using the full distribution of (2.11).

The above distributions take for granted that the advection speed can be split according to (2.9). For non-convex fluxes, a general flux splitting was proposed by Engquist and Osher [37], which can be expressed in $d^{\pm}$ as

$$f^{\pm}_{\mathrm{EO}}(u) = \int_0^u \pm d^{\pm}_{\xi} a(\xi)\,\mathrm{d}\xi = \int_0^u a^{\pm}_{\xi}\,\mathrm{d}\xi\,, \quad \text{with} \quad a(u) = f'(u). \tag{2.19}$$

For the interface flux see [37, 3]. This is a local splitting of the flux in f^+_i and f^-_i, and for reasons of consistency the parts can only be distributed with the local splitting of (2.11), resulting in the update of (2.13). However, we can compute $a^{\pm}_{\mathrm{EO}}(u_{i+1/2})$, and apply the cell-based split advection speeds to the distribution coefficients of (2.15) and to the FDS scheme of (2.16). The upwind speeds are

$$a^+_{\mathrm{EO}}(u) = \frac{\partial f^+}{\partial u} = \frac{\partial}{\partial u}\int_0^u a^+(\xi)\,\mathrm{d}\xi = \frac{\partial}{\partial u}\int_0^u \tfrac{1}{2}(a(\xi) + |a(\xi)|)\,\mathrm{d}\xi\,, \tag{2.20}$$

where the last integral has to be taken over the successive intervals between the sonic points, where $a(u)$ changes sign. In the absence of sonic points in the integration path, this is just the flux splitting of (2.9).

In the case of a flux function which is homogeneous in u, we can split $f_i = a_i u_i$ in positive and negative parts according to the sign of a_i or according to the methods just described.

Finally, we can construct a non-conservative distribution in the case of a homogeneous flux. Instead of distributing the flux $f_i = a_i u_i$, distribute $f_{i-1/2} = a_{i-1/2}u_i$ and $f_{i+1/2} = a_{i+1/2}u_i$ with (2.15). The result is

$$u_i^{n+1} - u_i^n = -\frac{\Delta t}{\Delta x}\left\{a^-_{i+1/2}(u_{i+1} - u_i) + a^+_{i-1/2}(u_i - u_{i-1})\right\}, \tag{2.21}$$

which is the characteristic scheme of Courant et al. [39] for the linear advection equation. The sum of the distributed fluxes is nonzero for the nonlinear equation.

The schemes of (2.13) and (2.16) have different behavior in capturing discontinuities of the solution. They are well-documented, see e.g. [2, 3]. The FDS captures discontinuities with less intermediate points than FVS, but allows non-physical expansion fans. The PDE of (2.1) has no viscous terms which prevent entropy decrease and therefore the solutions which violate the entropy inequality have to be excluded explicitly. The transonic expansion is characterized by $a_{i-1/2} < 0 < a_{i+1/2}$. This has the effect that node u_i does not change its value with the FVD discretization of (2.16). In the present formulation, this can easily be prevented by switching to a different scheme. The value of u_i will change when the local advection speed a_i is used in the update of (2.16), turning it into the FVS of (2.13). The switching of schemes has been proposed by Coquel and Liou [40].

Another option is to apply a sub-cell resolution scheme in the case that a sonic point is present in the region $(x_{i-1/2}, x_{i+1/2})$, see e.g. [41, 42]. If the position of the sonic point x_s is given by the parameter θ, with $\theta = 0$ for $x_s = x_{i-1/2}$, we can apply two distributions of the flux: the part θf_i with the left speed and $(1-\theta)f_i$ with the right speed. This avoids an expansion shock, and sharpens also the compression shock.

The central scheme. The distribution coefficients for the central scheme are

$$\alpha^i_{i-1} = \tfrac{1}{2}\,, \quad \alpha^i_i = 0\,, \quad \text{and} \quad \alpha^i_{i+1} = -\tfrac{1}{2}\,, \tag{2.22}$$

which are the same for the nodal and cell-wise distributions.

The Lax-Wendroff type schemes. We begin by defining the nodal CFL number ν_N and the cell CFL number ν_C which are limited by stability constraints. These numbers define the time step used in the update of the nodal value and the cell time step, given by

$$\Delta t_i = \nu_N \frac{\Delta x_i}{a_i}\,, \quad \text{and} \quad \Delta t_{i+1/2} = \nu_C \frac{\Delta x_{i+1/2}}{a_{i+1/2}}\,. \tag{2.23}$$

With the distribution coefficients

$$\alpha^i_{i-1} = \tfrac{1}{2}(1-\nu_C)\,, \quad \alpha^i_i = \nu_C\,, \quad \text{and} \quad \alpha^i_{i+1} = -\tfrac{1}{2}(1+\nu_C)\,, \tag{2.24}$$

the update becomes

$$\begin{aligned} u_i^{n+1} - u_i^n &= -\frac{\Delta t_i}{\Delta x_i}\,\left\{-\tfrac{1}{2}(1+\nu_C)f_{i-1} + \nu_C f_i + +\tfrac{1}{2}(1-\nu_C)f_{i+1}\right\} \\ &= -\frac{\Delta t_i}{\Delta x_i}\,\left\{\tfrac{1}{2}\left\{f_{i+1} - f_{i-1}\right\} - \tfrac{1}{2}\nu_C\left(f_{i+1} - 2f_i + f_{i-1}\right)\right\}\,, \end{aligned} \tag{2.25}$$

$$f_{i+1/2} = \tfrac{1}{2}\left\{f_{i+1} + f_i\right\} - \tfrac{1}{2}\nu_C\left(f_{i+1} - f_i\right)\,. \tag{2.26}$$

This version of the Lax-Wendroff scheme has been analyzed by Crumpton et al. [43], who find that the scheme is stable under the restrictions $\nu_N \le \nu_C$ and $\nu_N\nu_C < 1$. The transition between the central part and the advection dependent part is governed by the parameter ν_C. For $\nu_N = \nu_C$, the discretization of [21] is obtained.

We have seen that classical discretizations can be cast in a FVD formulation. Since the origin of residual distribution schemes [18], the distribution has been based on the cell based advection speed. The RD formulation of Roe [44] is the counterpart of his flux difference splitter [22], and is therefore tuned to the use of the cell advection speed of (2.5). It turns out that FVD is more general since it includes FVS.

2.2. The distribution for the advection equation with source term.

A small review of the treatment of source terms tells us how to incorporate the effect of a source in the flux which is distributed in a FVD scheme.

Sidilkover [45] considers Cartesian grids with a central treatment of the source term for the N scheme. A thorough analysis is given by Rudgyard [42], who distributes the residual which includes the source term. The idea of applying an upwind discretization to the source term can be found e.g. in [46, 47, 48]. Koren [47] supports the approach of including the source term in an extended advective flux for reasons of convergence. The approaches of Rudgyard and Koren are closely related.

Consider the scalar advection equation for $u(x,t)$ containing a source term,

$$\frac{\partial u}{\partial t} + \frac{\partial f}{\partial x} + s(u,x) = 0\,, \quad \text{or} \quad \frac{\partial u}{\partial t} + a\frac{\partial u}{\partial x} + s(u,x) = 0\,, \quad \text{with} \quad a = \frac{\partial f}{\partial u}\,, \tag{2.27}$$

with initial condition $u(x,0) = u_0(x)$. At the sonic point the source term vanishes since otherwise u becomes unbounded, and the problem becomes ill-posed. Rudgyard shows that this condition furnishes the missing information which can be used to prevent an expansion shock.

Due to the presence of the source term, monotonicity of the solution cannot be guaranteed even when a monotonicity preserving discretization is used. On a characteristic curve

$$x = c(t)\,, \quad \text{with} \quad \frac{\partial c}{\partial t} = \frac{\partial f}{\partial u}\,, \tag{2.28}$$

the solution u evolves due to the source term according to

$$\frac{Du}{Dt} = \frac{\partial u}{\partial t} + \frac{\partial f}{\partial x} = -s(u,x)\,. \tag{2.29}$$

It is possible to choose a variable which remains constant on the characteristic curve. When we define

$$\tilde{u} = u + S(u,x) \quad \text{with } S(u,x) \text{ such that} \quad \frac{\partial f(\tilde{u})}{\partial x} = \frac{\partial f(u)}{\partial x} + s(u,x)\,, \tag{2.30}$$

then we have

$$\frac{D\tilde{u}}{Dt} = \frac{\partial \tilde{u}}{\partial t} + \frac{\partial f(\tilde{u})}{\partial x} = 0\,. \tag{2.31}$$

This is the homogeneous equation for $\tilde{u}$ which we can solve with a monotonic discretization. The condition on S becomes clear in the linear case since it reduces to

$$a\frac{\partial S}{\partial x} = s(u,x)\,. \tag{2.32}$$

This is the relation proposed by Koren for improved convergence, $S = (1/a)\int s\,\mathrm{d}x$, and $a\tilde{u} = au + \Delta x S$ if $\int s\,\mathrm{d}x = S\Delta x$ as used by Sidilkover [45]. The source term S can then be joined with the space discretization of the flux, which corresponds to the distribution of the residual including the source term of Rudgyard. In general, an analytical expression for S is not available, and the only approach is a numerical integration of (2.32). Let us define nodal values

$$S_i = \frac{1}{\Delta x_i}\int_{x_{i-1/2}}^{x_{i+1/2}} \left(\frac{\partial f}{\partial u}\right)^{-1} s(u,x)\,\mathrm{d}x\,. \tag{2.33}$$

The effect of the flux f_i and source term S_i at node j are now $\delta u_j := \delta u_j - (\Delta t/l_j)\,\alpha_j^i\,(f_i + S_i)$ since the distribution is equivalent to a discretization of a space derivative. The value of $u_i + S_i$ now takes the rôle of $\tilde{u}$. In the case of the presence of a sonic point in the region around the node, a sub-cell distribution can be applied as explained before. The integral appearing in the formulation of the source term in (2.33) can be split in the parts $(x_{i-1/2}, x_i)$ and $(x_i, x_{i+1/2})$. This is useful if the advection speeds of both cells are used for the distribution.

2.3. The Flux Vector Distribution for systems of equations.

We illustrate the application of FVD to systems of equations with the Euler equations for fluid dynamics. The Euler equations in conservative and linear form are given by

$$\frac{\partial \mathbf{U}}{\partial t} + \frac{\partial \mathbf{F}}{\partial x} = \mathbf{0}\,, \quad \text{and} \quad \frac{\partial \mathbf{U}}{\partial t} + A\frac{\partial \mathbf{U}}{\partial x} = \mathbf{0}\,. \tag{2.34}$$

The conservative variables $\mathbf{U} = (\rho, \rho u, \rho E)^\tau$ and flux vector $\mathbf{F} = (\rho u, \rho u^2 + p, \rho u H)^T$ are expressed in the density ρ, the velocity u, the total specific energy E, the pressure $p = \rho(\gamma - 1)(E - {}^{u^2}/_2)$, and the total specific enthalpy $H = E + {}^{p}/_{\rho}$. The corresponding Jacobian matrix is $A = {}^{\partial \mathbf{F}}/_{\partial \mathbf{U}}$. The matrix A^{-1} exists with R and L the matrices of the right and left eigenvectors of A.

The Euler equations admit wave-like solutions which are the transport of entropy and acoustical disturbances with their respective advection speeds u, $u + c$, and $u - c$. The classical flux decomposition in three components using those speeds is

$$\mathbf{F} = u\,\rho\frac{\gamma - 1}{\gamma}\begin{pmatrix} 1 \\ u \\ {}^{u^2}/_2 \end{pmatrix} + (u + c)\,\frac{\rho}{2\gamma}\begin{pmatrix} 1 \\ u + c \\ H + c \end{pmatrix} + (u - c)\,\frac{\rho}{2\gamma}\begin{pmatrix} 1 \\ u - c \\ H - c \end{pmatrix}\,. \tag{2.35}$$

The integration which appears in the scalar flux computation of Engquist-Osher, (2.19), generalizes to a triple integral in the space of $\mathbf{U}$ for the Euler equations. The lower bound of the integration is the vacuum state $\mathbf{U} = \mathbf{0}$. This is not a valid state for the Euler equations, which are based on sufficient interactions between the particles which constitute the fluid. We take as ρ_E the density where the mean free path of the particles is sufficiently small to be able to define pressure and temperature in a meaningful way. The assumption is that the contribution to the flux for values of the density below ρ_E is negligible, which is easier to justify when the actual state with density ρ is far from rarefied. For the integration path in the triple integral we choose the path where u and E have the value of the final state, while integrating from $\rho_E \approx 0$ to ρ. This means that we keep $E - {}^{u^2}/_2$ and therefore the speed of sound constant. On the integration path, the Mach number is constant and the splitting in forward and backward flux only depends on the final state. The result is the splitting of (2.35).

Another integration path is along the Riemann invariants as originally proposed by Osher [49, 50]. The order of integration was changed from the O-variant to the P-variant by Hemker and Spekreijse [51] to improve efficiency. The integration from the vacuum state to the desired state $\mathbf{U}$ makes use of two intermediate states $\mathbf{U}_{1/3}$ and $\mathbf{U}_{2/3}$. The remaining two state variables at $\mathbf{U} = \mathbf{0}$ with $\rho = \rho_E$ are not determined, and lead to a two-parameter class of splittings.

For the distribution we can extend the directional coefficients d of (2.10) to directional matrices $D = A\,|A^{-1}|$. The flux components are then $D^{\pm}\mathbf{F} = R\Lambda^{\pm}LR|\Lambda|^{-1}L\mathbf{F}$, or the terms of (2.35).

If we distribute the flux components of (2.35) with the nodal advection speeds, we have the splitting of Steger and Warming [52].

When we distribute the flux components with the cell wise speeds, we base the computation of the factors u and $u \pm c$ in (2.35) on cell-averaged values, while the state vectors are computed with nodal values. Using the system version of the conservative linearization of (2.5),

$$\mathbf{F}_{i+1} - \mathbf{F}_i = A_{i+1/2}(\mathbf{U}_{i+1} - \mathbf{U}_i)\,, \tag{2.36}$$

we have the scheme of Roe [44].

The same flux splitting can therefore be used for generating FVS and FDS schemes depending on distributing the flux components with nodal or cell-wise velocities. This applies also to other decompositions than (2.35).

The extension to systems of equations of the non-conservative distribution of (2.21) gives the split coefficient matrix method of Chakravarthy et al. [53].

2.4. Extra nodes for higher order schemes.

We consider five point stencils for monotonic second order schemes with limiters in the spirit of [4, 54, 55, 56, 57, 5, 58].

For the FV method, we have two extrapolations at our disposal to arrive at a higher order estimate of the interface flux $f_{i\pm1/2}$. With variable extrapolation, the piecewise constant states are replaced by higher order variations. The arguments u_i and u_{i+1} of the numerical flux $f_{i\pm1/2}$ are replaced by the extrapolated values $u^L_{i+1/2}$ and $u^R_{i+1/2}$. The interface flux $f_{i\pm1/2}(u^L_{i+1/2}, u^R_{i+1/2})$, and hence the update, thus depend on a larger stencil. For monotonic results with FVS or FDS, the second order contributions are limited, $u^L_{i+1/2} = u_i + {}^1\!/_2\,\phi\,(r_i)\,[u_i - u_{i-1}]$ and $u^R_{i+1/2} = u_{i+1} - {}^1\!/_2\,\phi\,({}^1\!/_{r_{i+1}})\,[u_{i+2} - u_{i+1}]$. Here, r_i is the ratio of consecutive gradients [59], $r_i = {}^{\Delta_{i+1/2}u}\!/_{\Delta_{i-1/2}u} = {}^{(u_{i+1}-u_i)}\!/_{(u_i-u_{i-1})}$.

An alternative to variable extrapolation is flux extrapolation. For monotonic results with FVS, limiters are introduced on the extrapolated fluxes (see e.g. Hirsch [60]), leading to $f^L_{i+1/2} = f^+_i + {}^1\!/_2\,\phi\left(r^+_i\right)\left[f^+_i - f^+_{i-1}\right]$, and $f^R_{i+1/2} = f^-_{i+1} - {}^1\!/_2\,\phi\,({}^1\!/_{r^-_{i+1}})\left[f^-_{i+2} - f^-_{i+1}\right]$. Now, $r^\pm_i$ is the ratio of consecutive flux gradients [59, 60], $r^\pm_i = {}^{\Delta_{i+1/2}f^\pm}\!/_{\Delta_{i-1/2}f^\pm} = {}^{(f^\pm_{i+1} - f^\pm_i)}\!/_{(f^\pm_i - f^\pm_{i-1})}$. The update for FVS is then

$$u^{n+1}_i - u^n_i = -\frac{\Delta t}{\Delta x}\left\{f^L_{i+1/2} + f^R_{i+1/2} - f^L_{i-1/2} - f^R_{i-1/2}\right\}. \tag{2.37}$$

The flux computation is consistent since the numerical interface flux reverts to the physical flux in the case that all the arguments of the numerical flux are identical.

For linear advection, flux extrapolation reverts to variable extrapolation, which for the case $a > 0$ becomes

$$\begin{aligned} u^{n+1}_i - u^n_i = &- a\frac{\Delta t}{\Delta x}\left\{u^L_{i+1/2} - u^L_{i-1/2}\right\} = \\ &- a\frac{\Delta t}{\Delta x}\left\{u_i + \tfrac{1}{2}\,\phi_i(u_i - u_{i-1}) - u_{i-1} - \tfrac{1}{2}\,\phi_{i-1}(u_{i-1} - u_{i-2})\right\}, \end{aligned} \tag{2.38}$$

where $\phi_i = \phi\,(r_i)$. In smooth regions of the flow, the limiting functions ϕ have a value close to one. Only in regions of gradients ϕ can go to zero, resulting in a first order scheme. A Taylor series expansion on a grid with uniform spacing shows that

$$\begin{aligned} \frac{a}{\Delta x}\left(u^L_{i+1/2} - u^L_{i-1/2}\right) = &\left\{1 + \tfrac{1}{2}(\phi_i - \phi_{i-1})\right\} a\frac{\partial u}{\partial x} \\ &+ \tfrac{1}{2}\left\{-1 + \tfrac{1}{2}(3\phi_i - \phi_{i-1})\right\} a\frac{\partial^2 u}{\partial x^2}\Delta x + O(\Delta x^2). \end{aligned} \tag{2.39}$$

This is an inconsistent discretization of ${}^{a\partial u}\!/_{\partial x}$ with an error ${}^1\!/_2(\phi_i - \phi_{i-1}){}^{a\partial u}\!/_{\partial x}$. The condition for a consistent discretization is $\phi_i = \phi_{i-1}\ \forall i$. In the case that one flux is calculated with a second order extrapolation and the other flux with a first order extrapolation, the numerical method discretizes an advection equation with 0.5 or 1.5 times the desired

advection speed. The use of compressive limiters with values of ϕ exceeding the range $[0, 1]$ could even change the sign of a. Central schemes with a TVD artificial viscosity are equally concerned.

In practice, this inconsistency is absorbed in the time step. The temporal behavior is affected, but the effects are hardly noticeable. In the vicinity of a discontinuity, the scheme is first order, and the truncation error is of the order of Δx. Furthermore, the conservative formulation ensures respecting the Rankine-Hugoniot relations, and therefore the correct overall shock speed and strength. In the case of a shock, the advection speeds point toward the shock, and an error in the magnitude will not show up. This is not the case for an expansion fan. In extreme cases like a slowly moving shock, or near sonic points, one might expect some noticeable effects. The effect of a locally inconsistent scheme on the convergence needs investigation.

The update of (2.2) can be combined with a monotonic second order FDS. The interface flux contains limited contributions,

$$f^{(2)}_{i+1/2} = f_{i+1/2} + \tfrac{1}{2}\phi\left(r^+_i\right)\alpha^+_{i-1/2}(u_i - u_{i-1}) - \tfrac{1}{2}\phi\big(\frac{1}{r^-_{i+1}}\big)\alpha^-_{i+3/2}(u_{i+2} - u_{i+1})\,. \tag{2.40}$$

In the above, we have $r^\pm_i = a^\pm_{i+1/2}(u_{i+1} - u_i)/(a^\pm_{i-1/2}[u_i - u_{i-1}])$, with $f_{i+1/2}$ the first order flux of(2.4).

Higher order schemes can be obtained in various ways in the RD method. Similar to variable extrapolation with FV, the linear basis functions used in (2.6) can be replaced by higher order polynomials as explored e.g. in [61]. While this should work fine in one dimension, problems arise in more dimensions with the construction of the linearized advection speed [62], especially for systems of equations (in [61] the problem of linearization was not addressed). Another possibility, already indicated in [22], is the distribution of the residual to nodes further away. This corresponds to flux extrapolation in the FV method. In the following, we use the simplified notation $\phi^+_i = \phi\left(r^+_i\right)$ and $\phi^-_i = \phi\left(1/r^-_i\right)$. Consider RD with the second order coefficients ${}^{(2)}\alpha^{i+1/2}_j$ (see Fig. 2.5) :

$$\begin{aligned}
&{}^{(2)}\alpha^{i+1/2}_i = \left(1 + \tfrac{1}{2}\phi^-_i\right)\alpha^{i+1/2}_i\,, \quad {}^{(2)}\alpha^{i+1/2}_{i+1} = \left(1 + \tfrac{1}{2}\phi^+_{i+1}\right)\alpha^{i+1/2}_{i+1}\,,\\
&{}^{(2)}\alpha^{i+1/2}_{i-1} = -\tfrac{1}{2}\phi^-_i\,\alpha^{i+1/2}_i\,, \qquad {}^{(2)}\alpha^{i+1/2}_{i+2} = -\tfrac{1}{2}\phi^+_{i+1}\alpha^{i+1/2}_{i+1}\,.
\end{aligned} \tag{2.41}$$

The update procedure is the same as described in §2.1.2, but taking into account contributions from residuals further away. For all values of ϕ, the distribution coefficients add up to 1, and the scheme is conservative. The coefficients of (2.41) amount to an update of node i as indicated in Fig. 2.6. This corresponds to the second order FDS update, (2.2) and (2.40). A higher order extension of FVD can be obtained, like in the RD method, by means of changing the basis functions, or by distribution over nodes further away. For the moment we focus on a wider distribution stencil with second order coefficients ${}^{(2)}\alpha^i_j$ (see Fig. 2.7),

$$\begin{aligned}
{}^{(2)}\alpha^i_{i+2} &= -\tfrac{1}{2}\phi^+_{i+1}\alpha^i_{i+1}\,, & {}^{(2)}\alpha^i_{i+1} &= \left\{1 + \tfrac{1}{2}\left(\phi^+_i + \phi^+_{i+1}\right)\right\}\alpha^i_{i+1}\,,\\
{}^{(2)}\alpha^i_{i-2} &= -\tfrac{1}{2}\phi^-_{i-1}\alpha^i_{i-1}\,, & {}^{(2)}\alpha^i_{i-1} &= \left\{1 + \tfrac{1}{2}\left(\phi^-_i + \phi^-_{i-1}\right)\right\}\alpha^i_{i-1}\,,\\
{}^{(2)}\alpha^i_i &= \alpha^i_i - \tfrac{1}{2}\phi^+_i\alpha^i_{i+1} - \tfrac{1}{2}\,\phi^-_i\,\alpha^i_{i-1}\,.
\end{aligned} \tag{2.42}$$

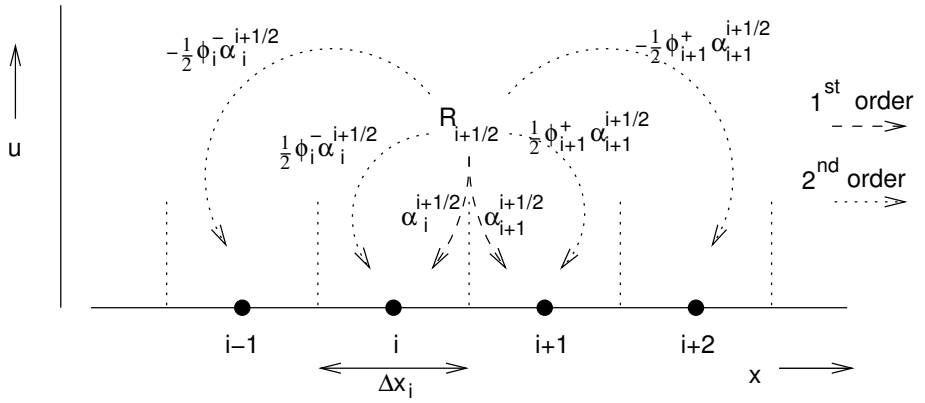

Figure 2.5. Distribution of the residual $R_{i+1/2}$ with coefficients for the 2^{nd} order RD scheme of (2.41).

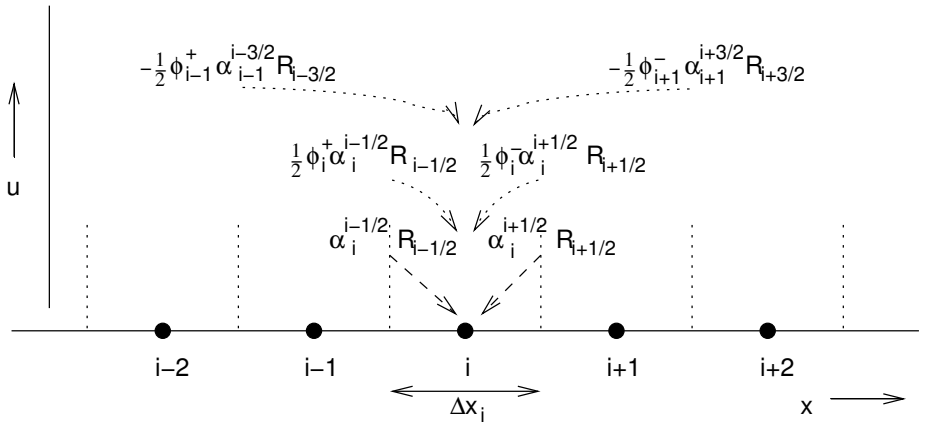

Figure 2.6. Update of node i with the 2^{nd} order RD scheme.

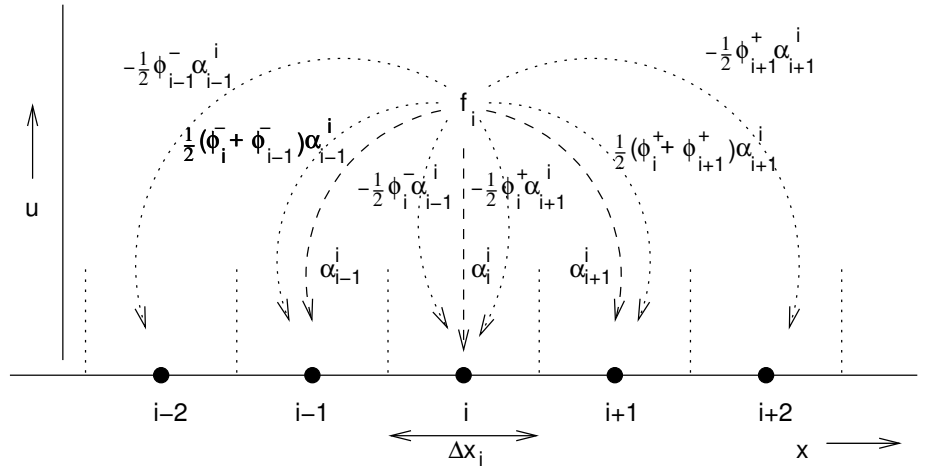

Figure 2.7. Distribution of the flux f_i with coefficients for the 2^{nd} order FVD scheme of (2.42).

The sum of the second order distribution coefficients is zero, as required for conservation. The update procedure is the same as described in §2.1.3, but taking into account

contributions from fluxes further away. The coefficients of (2.42) amount to an update of node i as indicated in Fig. 2.8. This corresponds to the second order FVS update, (2.37). Note that either α^i_{i-1} or α^i_{i+1} is zero, and thus the target nodes are either $i, i+1, i+2$ or $i, i-1, i-2$, dependent on the sign of a_i.

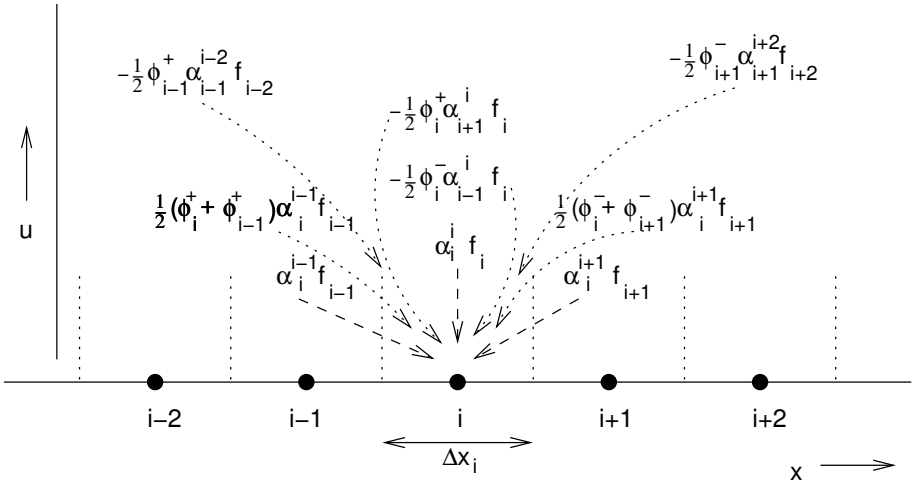

Figure 2.8. Update of node i with the 2^{nd} order FVD scheme.

3. Two-dimensional schemes in the Flux Vector Distribution formulation.

In this chapter we discuss the N scheme in the RD formulation on a grid consisting of triangles [21, 22], from which we will derive the FVD version. This is followed by schemes on structured grids with a consistency analysis.

The discretizations will be used to solve the scalar advection equation in nonlinear or linear form,

$$\frac{\partial u}{\partial t}+\frac{\partial f}{\partial x}+\frac{\partial g}{\partial y}=0\,,\quad \text{or}\quad \frac{\partial u}{\partial t}+a\frac{\partial u}{\partial x}+b\frac{\partial u}{\partial y}=0\,,\quad \text{with}\quad a=\frac{\partial f}{\partial u},\ b=\frac{\partial g}{\partial u}\,. \tag{3.1}$$

The N scheme is our point of departure because it is monotonic and it has a reduced grid dependency compared to the one-dimensional upwind scheme applied to each space direction. The one-dimensional schemes preserve a one-dimensional solution along the grid lines, while the N scheme is also exact along the diagonals of a quadrilateral on a structured grid. More general discretizations which can be expressed in the FVD formulation can be found in [35].

3.1. The Residual Distribution N scheme.

Define unknowns u at the nodes of a triangle of the grid. Opposite to node i is the edge i with an *inward* pointing edge normal vector $\vec{n}_i$, which has the length of edge i (Fig. 3.1a).

As a consequence, $\sum_{i=1}^{3}\vec{n}_i=\vec{0}$. The flux f_i through edge i is the dot product of the flux vector $\vec{f}=(f,g)^T$, the edge normal $\vec{n}_i$, $f_i=\vec{f}_i\cdot\vec{n}_i$, and the cell residual of triangle T is

$$R_T=\iint_{S_T}\vec{\nabla}\cdot\vec{f}\,\mathrm{d}x\,\mathrm{d}y\ =-\oint_{\partial T}\vec{f}\cdot\,\mathrm{d}\vec{n}\ =-\sum_{i=1}^{3}f_i\,. \tag{3.2}$$

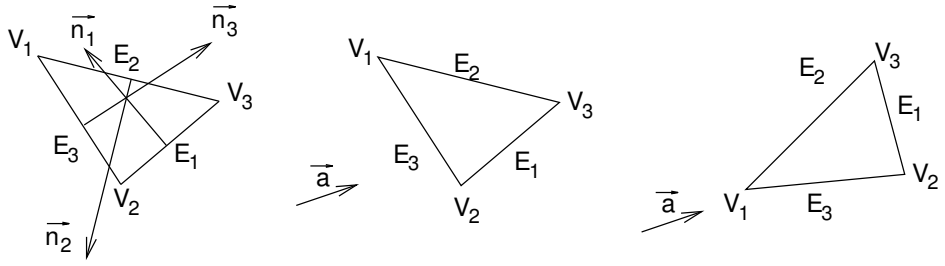

a) the edge normals b) one inflow side c) two inflow sides

Figure 3.1. Geometry of triangles with either one or two inflow sides.

The residuals R_T are distributed over the nodes of the triangles. Node i is updated like in one dimension (see §2.1.2) under the assumption of linear variation of u over the cell,

$$u_i^{n+1} = u_i^n - \frac{\Delta t}{S_{Di}} \sum_T \alpha_i^T R_T \,. \tag{3.3}$$

If the variation of u is not linear, the update formula changes, but like in the FE method, mass lumping can be applied. The term S_{Di} is the dual volume associated to node i and α_i^T is the weight with which the cell residual R_T is distributed to node i. Taking $\sum_{i=1}^3 \alpha_i^T = 1 \,\forall\, T$ means that the residuals are completely distributed, and that the scheme is conservative. Additional constraints can be imposed on the distribution coefficients α_i^T to provide e.g. monotonicity or linearity preservation. The schemes use the cell-based advection speed $\vec{a} = (a, b)^T$, and the distribution depends now on a_i or d_i, where $a_i = \vec{a} \cdot \vec{n}_i$, and $d_i = {}^{a_i}/_{|a_i|}$.

For upwind schemes like the N scheme, distribution is to the downwind nodes only. Two types of configurations are encountered (Fig. 3.1). Take e.g. $d_1 < 0$, $d_2 < 0$, and $d_3 > 0$ which means that the flow enters through one edge, E_3. The residual is distributed to the downwind node V_3 which means that

$$\alpha_3 = 1 \,, \quad \alpha_1 = \alpha_2 = 0 \,, \quad \text{and} \quad \delta u_3 := \delta u_3 - \frac{\Delta t}{S_3} R_T \,. \tag{3.4}$$

In the case where the flow enters through two edges of the triangle, $d_1 < 0$, $d_2 > 0$ and $d_3 > 0$, the distribution is to the two downstream nodes V_2 and V_3. In the linear case, the distribution is for the N scheme

$$\delta u_2 := \delta u_2 - \frac{\Delta t}{S_2} \tfrac{1}{2} a_2 (u_2 - u_1) \,, \quad \delta u_3 := \delta u_3 - \frac{\Delta t}{S_3} \tfrac{1}{2} a_3 (u_3 - u_1) \,. \tag{3.5}$$

The distribution of (3.4)–(3.5) has been generalized by Bourgois and Deconinck [63] to D dimensions as

$$\delta u_i := \delta u_i - \frac{\Delta t}{S_{Di}} \frac{a_i}{D \sum_{l=1}^{D+1} a_l^+} \sum_{j=1}^{D+1} a_j^- (u_j - u_i) \,. \tag{3.6}$$

For a suitable time step the scheme is monotone, as follow from (3.6) (see [22, 26] for details).

For the nonlinear advection equation an extension of (2.5) is

$$\vec{\nabla} \cdot f = \vec{a}_C \cdot \vec{\nabla} u \,. \tag{3.7}$$

Under the assumption of linear variation of u over the cell,

$$\iint_{S_T} \vec{\nabla} \cdot \vec{f}\,\mathrm{d}x\,\mathrm{d}y \;= \iint_{S_T} \vec{a} \cdot \vec{\nabla} u\,\mathrm{d}x\,\mathrm{d}y \;= \vec{\nabla} u \cdot \iint_{S_T} \vec{a}\,\mathrm{d}x\,\mathrm{d}y \;= \vec{a}_C \cdot \vec{\nabla} u\,, \tag{3.8}$$

and $\vec{a}_C = {}^1\!/_{S_T} \iint (\partial f/\partial u, \partial g/\partial u)^T \,\mathrm{d}S = \left(\partial f/\partial u|_{u_C}\,, \partial g/\partial u|_{u_C} \right)^T = \vec{a}(u_C)$. This advection speed can then be used in the distribution of (3.4)–(3.5).

The N scheme can be applied to a structured grid as indicated in Fig. 3.2.

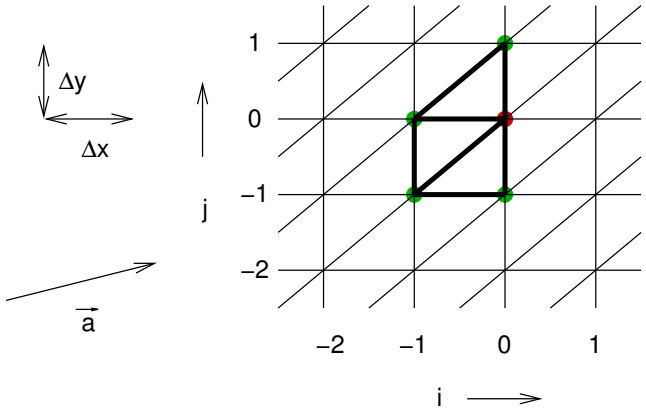

Figure 3.2. The structured triangular grid for the derivation of a first order N scheme. The triangles and nodes are indicated which contribute to $u_{0,0}$.

We consider the case $a\Delta y > b\Delta x > 0$, which means that the direction of the advection vector $\vec{a}$ is between the x-axis and the $y = x$ diagonal. Other advection directions follow by a permutation. For the linear advection equation, the resulting structured N scheme is

$$u_{0,0}^{n+1} = u_{0,0}^{n} - \frac{a\Delta t}{\Delta x}\left(u_{0,0} - u_{-1,0}\right) - \frac{b\Delta t}{\Delta y}\left(u_{-1,0} - u_{-1,-1}\right)\,, \tag{3.9}$$

see e.g. [45, 64]. When the diagonals in Fig. 3.2 are swapped, the resulting scheme is the one-dimensional grid-aligned upwind scheme for each coordinate direction. The N scheme has lesser cross-diffusion than the one-dimensional grid-aligned upwind scheme, since it also captures a one-dimensional flow along a diagonal. This is easily shown by a transformation to streamline coordinates, see e.g. [45, 65, 14, 64, 35]. When the flow is along the diagonal, $a\Delta y = b\Delta x$, the node $(-1, 0)$ disappears from the discretization, and the only points involved in the update are on the diagonal. This is further exploited in [35] for the construction of higher order diagonal discretizations in any number of dimensions.

The N scheme is consistent on a regular triangulation like the one shown in Fig. 3.2. It loses consistency locally in different grid configurations. Figure 3.3 shows an example of a grid on which the first order N scheme is inconsistent.

The vertices are surrounded either by four or eight triangles, resulting in a different numerical scheme for each node. For the node surrounded by four triangles, the update is given by

$$\frac{2}{3}\frac{\Delta x \Delta y}{\Delta t}\left(u_{0,0}^{n+1} - u_{0,0}^{n}\right) = -\frac{a}{\Delta x}\left(u_{0,0} - u_{-1,0}\right) - \frac{b}{2\Delta y}\left(u_{-1,0} - u_{0,-1}\right)\,, \tag{3.10}$$

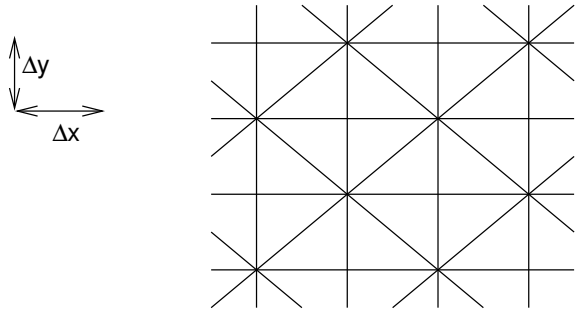

Figure 3.3. A structured triangular grid with either four or eight triangles meeting at a vertex.

and for the node surrounded by eight triangles by

$$\frac{4}{3}\frac{\Delta x\Delta y}{\Delta t}\left(u_{0,0}^{n+1}-u_{0,0}^{n}\right)=-\frac{a}{\Delta x}\left(u_{0,0}-u_{-1,0}\right) \\ -\frac{b}{\Delta y}\left(u_{0,0}+\tfrac{1}{2}u_{-1,0}-u_{-1,-1}-\tfrac{1}{2}u_{0,-1}\right). \qquad (3.11)$$

The left hand side of the above equations contains the dual surface surrounding the node, while the right hand side is a numerical approximation for the advection term $-\vec{a}.\vec{\nabla}u$. When the nodal values are developed in a Taylor series around $u_{0,0}$, the updates become respectively

$$\frac{2}{3}\frac{\Delta x\Delta y}{\Delta t}\left(u_{0,0}^{n+1}-u_{0,0}^{n}\right)=-\left(a-b\frac{\Delta x}{2\Delta y}\right)\frac{\partial u}{\partial x}-\frac{1}{2}b\frac{\partial u}{\partial y}+O\left(\Delta x,\Delta y,\frac{(\Delta x)^2}{\Delta y}\right),$$

and

$$\frac{4}{3}\frac{\Delta x\Delta y}{\Delta t}\left(u_{0,0}^{n+1}-u_{0,0}^{n}\right)=-\left(a+b\frac{\Delta x}{2\Delta y}\right)\frac{\partial u}{\partial x}-\frac{3}{2}b\frac{\partial u}{\partial y}+O\left(\Delta x,\Delta y,\frac{(\Delta x)^2}{\Delta y}\right). \qquad (3.12)$$

Evidently, both discretizations are inconsistent.

It is possible to define flux functions which produces the N scheme in a FV discretization. The fluxes through the edges of the dual volume of the nodes are

$$\text{for one inflow}\begin{cases} f_{e_1}= f(u_{e2}),\\ f_{e_2}= f(u_{e1}),\\ f_{e_{t2}}= f(u_{t1}),\end{cases}\quad\text{and for two inflow}\quad\begin{cases} f_{e_1}= f(u_{e1}),\\ f_{e_2}= f(u_{e1}),\\ f_{e_{t2}}= f(u_{e1}),\end{cases} \qquad (3.13)$$

see Fig. 3.4. On the regular grid of Fig. 3.2, this gives back the N scheme. The fluxes are discontinuous functions of the flow angle.

The central discretization is consistent on the grid of Fig. 3.3.

3.2. The Flux Vector Distribution N scheme.

We rewrite the distribution of the residual with the N scheme as a distribution of the fluxes. We use the notation of the previous section. The update formula to advance node i in time under the effect of the contributing fluxes is

$$u_i^{n+1}=u_i^n-\frac{\Delta t}{S_{Di}}\sum_j \alpha_i^j f_j\,. \qquad (3.14)$$

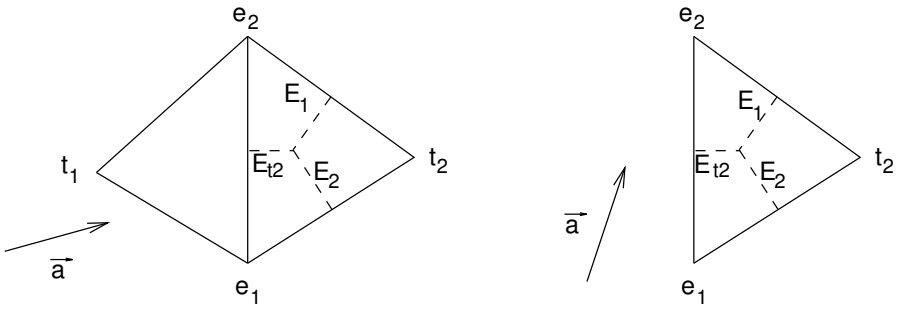

a) flow enters the right triangle through one side b) entering through two sides

Figure 3.4. The names of the edges which are used in the FV formulation correspond to the opposite nodes in the triangle.

This is the two-dimensional version of (2.8), and similar to (3.3), except for the distribution of fluxes with their coefficients.

In the one-target case when the flow enters the triangle through one side only, all fluxes f_i are simply sent to the downstream node V_3. The downstream distribution, (3.4), becomes in the flux distribution $\delta u_3 := \delta u_3 + ({}^{\Delta t}/_{S_3}) \sum_{i=1}^{3} f_i$ with coefficients

$$\alpha_3^1 = \alpha_3^2 = \alpha_3^3 = -1\,. \tag{3.15}$$

We rewrite the two-target linear case of (3.5) as

$$\delta u_2 := \delta u_2 - \frac{\Delta t}{S_2}\,(\frac{a_2}{a_1} f_1 - f_2)\,, \quad \delta u_3 := \delta u_3 - \frac{\Delta t}{S_3}\,(\frac{a_3}{a_1} f_1 - f_3)\,, \tag{3.16}$$

The two terms $({}^{a_2}/_{a_1} f_1 - f_2)$ and $({}^{a_3}/_{a_1} f_1 - f_3)$ add up to R_T, (3.2). The FVD distribution coefficients in this case can be written as

$$\alpha_2^1 = \frac{a_2}{a_1}, \quad \alpha_3^1 = \frac{a_3}{a_1}, \quad \alpha_2^2 = \alpha_3^3 = -1\,. \tag{3.17}$$

The update in D dimensions is in compact form

$$\delta u_i := \delta u_i - \frac{\Delta t}{S_{Di}} \left\{ -d_i \vec{f}_i \cdot \vec{n}_i - \frac{a_i}{\sum_{l=1}^{D+1} a_l^+} \left(\sum_{j=1}^{D+1} d_j^- \vec{f}_j \cdot \vec{n}_j \right) \right\}\,, \tag{3.18}$$

which is a generalization of (2.16).

The above coefficients are used for the three fluxes of a triangle. In an implementation of a FVD scheme, the distribution loop is over the edges of the grid. We need therefore a distribution formula for the flux of each edge between two triangles. In Fig. 3.5, a general layout is shown for the case that the flow enters the right triangle through edge e between nodes e_1 and e_2. The edge normal $\vec{n}_e$ is pointing to the right, and $a_e = \vec{a} \cdot \vec{n}_e > 0$.

Concerning the right triangle, for both the one-inflow or two-inflow case, the flux $f_e = \vec{f}_e \cdot \vec{n}_e$ goes to node t_2, and $\alpha_{t_2}^e = -1$. With respect to the left triangle, we have to take care of the signs, since the convention of Fig. 3.1 assumes inward pointing normals. Dependent on the direction of $\vec{a}_e$ with respect to the edges l_1 between vertices t_1 and e_2,

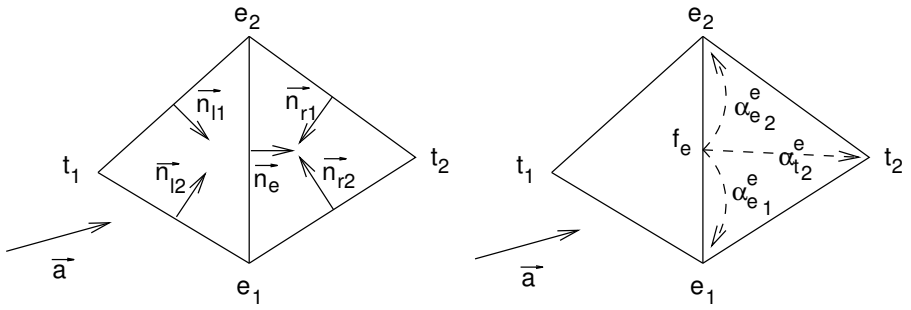

Figure 3.5. The FVD scheme in an edge-based context. For clarity sake the normals have been drawn too small. Left : the geometry. Right : the distribution of the edge flux.

and l_2 between vertices t_1 and e_1, the distribution is towards nodes e_1 and e_2 :

$$\alpha^e_{e_1} = \begin{cases} 0 & \text{for } \vec{a}\cdot\vec{n}_{l_1} < 0 \\ \dfrac{a_{l_1}}{a_e} & \text{for } \vec{a}\cdot\vec{n}_{l_1} > 0 \text{ and } \vec{a}\cdot\vec{n}_{l_2} > 0\,, \\ 1 & \text{for } \vec{a}\cdot\vec{n}_{l_2} < 0 \end{cases} \qquad \alpha^e_{e_2} = \begin{cases} 1 & \text{for } \vec{a}\cdot\vec{n}_{l_1} < 0 \\ \dfrac{a_{l_2}}{a_e} & \text{for } \vec{a}\cdot\vec{n}_{l_1} > 0 \text{ and } \vec{a}\cdot\vec{n}_{l_2} > 0\,. \\ 0 & \text{for } \vec{a}\cdot\vec{n}_{l_2} < 0 \end{cases} \tag{3.19}$$

In all the cases, the sum adds up to zero as required for conservation. Remark the similarity with the schemes of §2.1.3, where for $a > 0$ $\alpha^i_{i-1} = 0$, $\alpha^i_i = 1$, and $\alpha^i_{i+1} = -1$. Here, $\alpha^e_{t_1} = 0$, $\alpha^e_{e_1} + \alpha^e_{e_2} = 1$, and $\alpha^e_{t_2} = -1$. The one-dimensional grid-aligned central scheme is recovered using weights $\alpha^e_{t_1} = -1/3$, $\alpha^e_{t_2} = 1/3$, and $\alpha^e_{e_1} = \alpha^e_{e_1} = 0$.

The N scheme is based on a cell-averaged advection speed for the non-linear case. In the FVD formulation we have the options of §2.1.3. For distribution with the cell-based advection speed we can choose an average of the advection speeds at the nodes, or an average of the advection speeds at the edges, of the advection speeds computed from the average of the nodal unknowns,

$$\vec{a}_C = \frac{1}{D+1}\sum_{i=1}^{D+1}\left.\frac{\partial\vec{f}}{\partial u}\right|_i\,, \quad \text{or} \quad \vec{a}_C = \frac{1}{D+1}\sum_{i=1}^{D+1}\left.\frac{\partial\vec{f}}{\partial u}\right|_{\text{edge } i}\,, \quad \text{or} \quad \vec{a}_C = \left.\frac{\partial\vec{f}}{\partial u}\right|_{u_C}\,, \tag{3.20}$$

where $u_C = 1/(D+1)\sum_{i=1}^{D+1} u_i$ is the cell averaged unknown. The third choice of (3.20) leads to a generalization of the method of Huang [38], while the advection speed of (3.7) is a generalization of the splitting of Roe [22].

Distribution of the edge flux with cell-averaged advection speeds implies that the averaged advection speeds on both sides of the edge are involved, like in §2.1.3.

The distribution with edge-based advection speeds leads to a directional generalization of the FVS method.

3.3. A Flux Vector Distribution scheme in Finite Volume context.

Instead of positioning the unknowns at the vertices of the triangles, a more FV like approach can be taken when the unknowns are edge-centered. This is indicated in Fig. 3.6 for triangles with one and two inflow sides. Also shown is the dual volume around the unknowns. The dual volumes are now quadrilaterals, with two corners at the vertices of the triangle, and two meeting in the gravity centers of the triangles. We define the inward pointing normals such that $\vec{n}_1$ is normal to the edge on which node V_1 is situated. The

residual in the linear case is $R_T = -\vec{a}\cdot\sum_i u_i\vec{n}_i = -\sum_i \vec{f}_i\cdot\vec{n}_i = -\sum_i f_i$. In the two-inflow case (Fig. 3.6b) the residual goes to node 2, $\delta u_2 := \delta u_2 - (\Delta t/S_2)\, R_T$. In the one-inflow case (Fig. 3.6a) we distribute similar to (3.16),

$$\begin{aligned}
\delta u_2 &:= \delta u_2 - \frac{\Delta t}{S_2}\,\vec{a}\cdot\vec{n}_2(u_1-u_2) = \delta u_2 - \frac{\Delta t}{S_2}\left(\frac{\vec{a}\cdot\vec{n}_2}{\vec{a}\cdot\vec{n}_1}f_1 - f_2\right),\\
\delta u_3 &:= \delta u_3 - \frac{\Delta t}{S_3}\,\vec{a}\cdot\vec{n}_3(u_1-u_3) = \delta u_3 - \frac{\Delta t}{S_3}\left(\frac{\vec{a}\cdot\vec{n}_3}{\vec{a}\cdot\vec{n}_1}f_1 - f_3\right).
\end{aligned} \tag{3.21}$$

A further analysis of this scheme shows that the resulting discretization is inconsistent with the original partial differential equation, (3.1). This edge-based data structure will not be further considered.

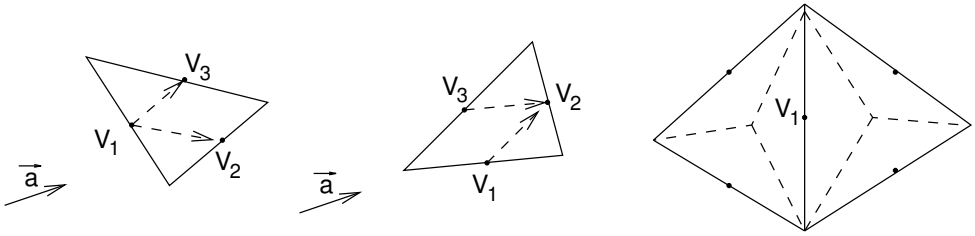

a) one inflow side b) two inflow sides c) dual volume around edge-centered node V_1

Figure 3.6. The FVD scheme in an edge-based context ; geometry of triangles with either one or two inflow sides.

3.4. The Flux Vector Distribution for systems of equations.

We take again the example of the Euler equations in conservative and linear form,

$$\frac{\partial \mathbf{U}}{\partial t} + \frac{\partial \mathbf{F}}{\partial x} + \frac{\partial \mathbf{G}}{\partial y} = \mathbf{0}\,, \quad \text{and} \quad \frac{\partial \mathbf{U}}{\partial t} + A\frac{\partial \mathbf{U}}{\partial x} + B\frac{\partial \mathbf{U}}{\partial y} = \mathbf{0}\,. \tag{3.22}$$

The conservative variables and fluxes in x and y direction are $\mathbf{U} = (\rho, \rho u, \rho v, \rho E)^\tau$ with u and v the velocity components, $\mathbf{F} = (\rho u, \rho u^2 + p, \rho uv, \rho uH)^T$, and $\mathbf{G} = (\rho u, \rho uv, \rho v^2 + p, \rho uH)^T$ respectively. The corresponding non-commuting Jacobian matrices A and B are $A = \partial\mathbf{F}/\partial\mathbf{U}$ and $B = \partial\mathbf{G}/\partial\mathbf{U}$. Given $\vec{n}$ a unit vector, the vectors $\mathbf{r}_k$ are right eigenvectors of $C_n = An_x + Bn_y$, related to entropy, shear, and acoustic wave components.

Following common practice we can decompose $\mathbf{U}$ in this base,

$$\mathbf{U} = \begin{pmatrix}\rho\\ \rho u\\ \rho v\\ \rho E\end{pmatrix} = \rho\,\frac{\gamma-1}{\gamma}\begin{pmatrix}1\\ u\\ v\\ \frac{1}{2}(u^2+v^2)\end{pmatrix} + \frac{\rho}{2\gamma}\begin{pmatrix}1\\ u+cn_x\\ v+cn_y\\ H+cu_n\end{pmatrix} + \frac{\rho}{2\gamma}\begin{pmatrix}1\\ u-cn_x\\ v-cn_y\\ H-cu_n\end{pmatrix}, \tag{3.23}$$

where $u_n = \vec{u}\cdot\vec{n}$. From the individual components of (3.23) we compute the flux components $\mathbf{F} = A\mathbf{U}$ and $\mathbf{G} = B\,\mathbf{U}$. The individual components of the edge flux can then be distributed according to the proper advection speed, leaving the choice for cell-averaged or edge-based speeds.

The system version of the conservative linearization ((3.7)) uses the parameter vector $\mathbf{Z} = (z_1, z_2, z_3, z_4)^\tau = \sqrt{\rho}(1, u, v, H)^\tau$ which varies linearly over the triangle [66, 26, 62]. This allows us to write with $\vec{\mathbf{F}} = (\mathbf{F}, \mathbf{G})^T$ and $\vec{A} = (A, B)^T$,

$$\widehat{\vec{\nabla} \cdot \vec{\mathbf{F}}} = \overline{\vec{A}} \cdot \widehat{\vec{\nabla}\mathbf{U}} = \overline{A}\, \frac{\widehat{\partial \mathbf{U}}}{\partial x} + \overline{B}\, \frac{\widehat{\partial \mathbf{U}}}{\partial y}\,. \tag{3.24}$$

The notation $\widehat{...}$ is a reminder that the gradients are based on a linearly varying $\mathbf{Z}$, while $\overline{...}$ indicates that the expression is evaluated at the averaged state $\overline{\mathbf{Z}} = {}^1\!/_3 \sum_i \mathbf{Z}_i$. While in the one-dimensional case the linearization can be based on linearly varying primitive variables [67, 68], the only reasonable candidate in two and three dimensions is the parameter vector $\mathbf{Z}$ [62].

Based on the conservative linearization, we can write for the flux through an edge of a triangle, e.g. edge 3,

$$\tfrac{1}{2}(\vec{\mathbf{F}}_1 + \vec{\mathbf{F}}_2) \cdot \vec{n}_3 = C_3 \tfrac{1}{2}(\mathbf{U}_1 + \mathbf{U}_2)\,, \tag{3.25}$$

with $C_3 = \vec{A} \cdot \vec{n}_3 = (A, B)^T \cdot \vec{n}_3$. This flux can be distributed in a FVD scheme, illustrating that RD matrix distribution schemes [69, 30, 31] can be accommodated in the FDV formulation.

3.5. Higher order Flux Vector Distribution schemes.

Like in one dimension, we increase the order of the N scheme by distributing the edge flux to nodes further downstream. We have to recalculate the distribution coefficients to obtain consistent higher order schemes. We will start with the FVD formulation, leading to RD expressions.

3.5.1. The second order Flux Vector Distribution N scheme.

We start with the stencil of Fig. 3.5 to which we add the closest downstream nodes r_1 and r_2, see Fig. 3.7. With this stencil, a second order scheme can be constructed. It is not necessary to include nodes on the right of t_2.

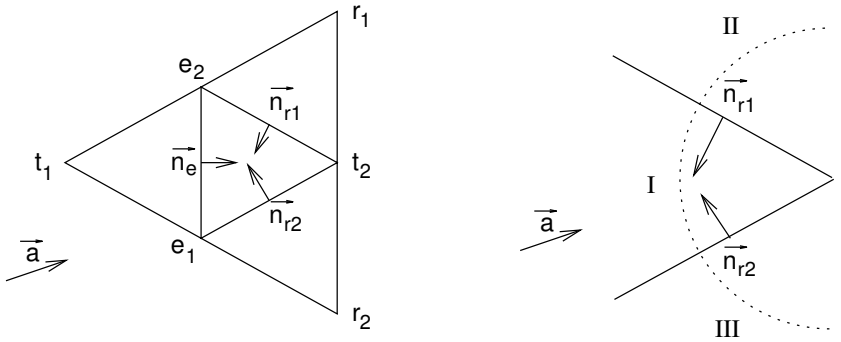

Figure 3.7. a) The stencil for a second order FVD scheme. b) the weather-vane for target nodes r_1 and r_2.

Like before, we consider the case that the flow enters the right center triangle through edge e, with $a_e > 0$. We distinguish three types of flux receiving nodes: a) e_1 and e_2 with distribution coefficients $\alpha^e_{e_1}$ and $\alpha^e_{e_2}$; b) t_2 with distribution coefficient $\alpha^e_{t_2}$; c) r_1 and r_2 with distribution coefficients $\alpha^e_{r_1}$ and $\alpha^e_{r_2}$. For category a) and b), we take the first order coefficients of (3.17) and (3.15), multiplied by factors C_E and C_T respectively, which will

be determined below. For the remaining downstream nodes, using a factor C_R, the desired coefficients must contain information of the angle between the advection speeds and the normals, like the first order coefficients, or like the coefficients of (3.21). In Fig. 3.7b, three domains have been indicated in the weather-vane associated with $\vec{a}$. If $\vec{a}$ falls in sector II, we send f_e to node r_2 ; if $\vec{a}$ falls in sector III, we send f_e to node r_1. In sector I, we use the distribution coefficients $\alpha^e_{r_1} = {}^{a_{r_1}}/_{a_e}$ and $\alpha^e_{r_2} = {}^{a_{r_2}}/_{a_e}$. In summary, the coefficients are

$$\alpha^e_{r_1} = \begin{cases} 0 & \text{for } \vec{a}\cdot\vec{n}_{r_1} > 0 \\ \dfrac{\vec{f}_e\cdot\vec{n}_{r_1}}{\vec{f}_e\cdot\vec{n}_e} & \text{for } \vec{a}\cdot\vec{n}_{r_1} < 0 \text{ and } \vec{a}\cdot\vec{n}_{r_2} < 0\,, \\ -1 & \text{for } \vec{a}\cdot\vec{n}_{r_2} > 0 \end{cases}$$

$$\alpha^e_{r_2} = \begin{cases} -1 & \text{for } \vec{a}\cdot\vec{n}_{r_1} > 0 \\ \dfrac{\vec{f}_e\cdot\vec{n}_{r_2}}{\vec{f}_e\cdot\vec{n}_e} & \text{for } \vec{a}\cdot\vec{n}_{r_1} < 0 \text{ and } \vec{a}\cdot\vec{n}_{r_2} < 0\,. \\ 0 & \text{for } \vec{a}\cdot\vec{n}_{r_2} > 0 \end{cases} \tag{3.26}$$

The conservation condition, $\sum_j \alpha^i_j = 0$, now becomes

$$C_E\left\{\alpha^e_{e1} + \alpha^e_{e2}\right\} + C_T\alpha^e_{t2} + C_R\left\{\alpha^e_{r_1} + \alpha^e_{r_2}\right\} = 0\,, \quad \text{or} \quad C_E - C_T - C_R = 0\,. \tag{3.27}$$

The above scheme is easiest analyzed on a structured grid with spacings Δx and Δy and with the three possible edge normal vectors $\vec{n}_1 = \binom{-\Delta y}{0}$, $\vec{n}_2 = \binom{\Delta y}{-\Delta x}$ and $\vec{n}_3 = \binom{0}{\Delta x}$, as shown in Fig. 3.8. We consider the case $a\Delta y > b\Delta x > 0$, which means that the advection vector $\vec{a}$ lies between the x-axis and the $y = x$ diagonal.

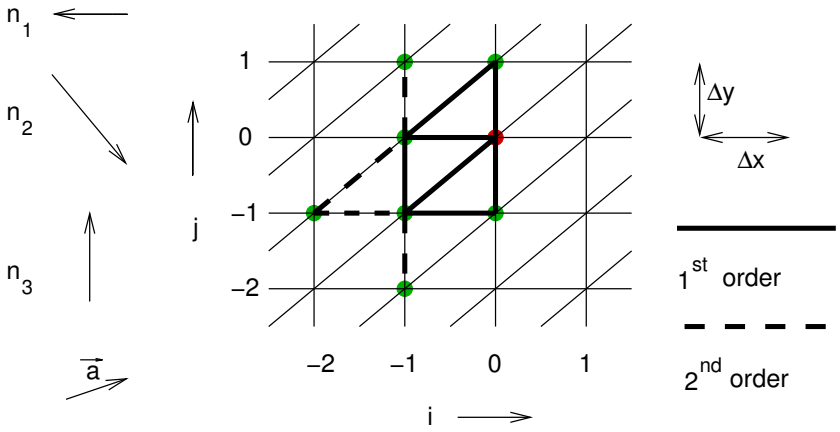

Figure 3.8. The structured triangular grid with the three possible edge normal vectors $\vec{n}_1$, $\vec{n}_2$, and $\vec{n}_3$, for the derivation of a second order FVD N scheme. The edges and vertices are indicated which contribute to $u_{0,0}$.

As a short notation for the fluxes, take for the flux through a horizontal edge $\vec{f}_{i+1/2,j} = \vec{f}((i+1/2)\Delta x, j\Delta y) = \vec{a}\,{}^1\!/_2\,(u_{i,j} + u_{i+1,j})$, through a vertical edge $\vec{f}_{i,j+1/2} = \vec{f}(i\Delta x, (j+1/2)\Delta y) = \vec{a}\,{}^1\!/_2\,(u_{i,j} + u_{i,j+1})$, and through a diagonal $\vec{f}_{i+1/2,j+1/2} = \vec{f}((i+1/2)\Delta x, (j+1/2)\Delta y) = \vec{a}\,{}^1\!/_2\,(u_{i,j} + u_{i+1,j+1})$. The analysis is simplified by using a program which

handles symbolic manipulation, like MuPAD [70]. The fluxes contribute in the following way to the update of $u_{0,0}$, which is an approximation for $-\vec{a}\cdot\vec{\nabla}u$, as:

$$\begin{aligned}-(\Delta x\Delta y)\vec{a}\cdot\vec{\nabla}u =& C_E\left(-\vec{f}_{0,1/2}\cdot\vec{n}_2+\vec{f}_{-1/2,0}\cdot(-\vec{n}_3)+\vec{f}_{-1/2,-1/2}\cdot(-\vec{n}_2)-\vec{f}_{0,-1/2}\cdot\vec{n}_3\right)+\\ & C_T\left(\vec{f}_{-1/2,1/2}\cdot\vec{n}_2+\vec{f}_{-1,-1/2}\cdot(-\vec{n}_1)+\vec{f}_{-1/2,-1}\cdot\vec{n}_3\right)+\\ & C_R\left(\vec{f}_{-1,1/2}\cdot\vec{n}_2+\vec{f}_{-1,-3/2}\cdot\vec{n}_3+\vec{f}_{-3/2,-1/2}\cdot\vec{n}_2+\vec{f}_{-3/2,-1}\cdot\vec{n}_3\right).\end{aligned} \tag{3.28}$$

When $C_E = C_T = 1$ and $C_R = 0$ we have the first order N scheme. For the second order scheme, the only nodes contributing to an update of $u_{0,0}$ are: $u_{-2,-1}$, $u_{-1,-2}$, $u_{-1,-1}$, $u_{-1,0}$, $u_{-1,1}$, $u_{0,-1}$, $u_{0,0}$, and $u_{0,1}$. We develop the nodal values of (3.28) in a Taylor series to obtain

$$\begin{aligned}-\vec{a}\cdot\vec{\nabla}u =& \frac{a}{2}\left(C_E-5C_R-3C_T\right)\frac{\partial u}{\partial x}+\frac{b}{2}\left(C_E-5C_R-3C_T\right)\frac{\partial u}{\partial y}+\\ & \frac{a}{4}\left(-C_E+7C_R+3C_T\right)\Delta x\frac{\partial^2 u}{\partial x^2}+\\ & \left[\left(C_E+5C_R+C_T\right)+\frac{a\Delta y}{2\Delta x}\left(-C_E+C_R+C_T\right)\right]\Delta y\frac{\partial^2 u}{\partial y^2}+\\ & \left[\left(C_E+5C_R+C_T\right)\Delta x+\frac{a}{2}\left(-C_E+C_R+C_T\right)\Delta y\right]\frac{\partial^2 u}{\partial x\,\partial y}+\\ & O\left(\Delta x^2,\Delta x\Delta y,\Delta y^2\right).\end{aligned} \tag{3.29}$$

With the conservation condition, (3.27),

$$\begin{aligned}-\vec{a}\cdot\vec{\nabla}u =& -a\left(2C_R+C_T\right)\frac{\partial u}{\partial x}-b\left(2C_R+C_T\right)\frac{\partial u}{\partial y}+\frac{a}{2}\left(3C_R+C_T\right)\Delta x\frac{\partial^2 u}{\partial x^2}+\\ & \frac{b}{2}\left(3C_R+C_T\right)\Delta y\frac{\partial^2 u}{\partial y^2}+b\left(3C_R+C_T\right)\Delta x\frac{\partial^2 u}{\partial x\,\partial y}+O\left(\Delta x^2,\Delta x\Delta y,\Delta y^2\right).\end{aligned} \tag{3.30}$$

For consistency, we need $2C_R + C_T = 1$, which reduces (3.30) to

$$\begin{aligned}-\vec{a}\cdot\vec{\nabla}u =& -a\frac{\partial u}{\partial x}-b\frac{\partial u}{\partial y}-\left(C_T-3\right)\left[\frac{a}{4}\Delta x\frac{\partial^2 u}{\partial x^2}+\frac{b}{4}\Delta y\frac{\partial^2 u}{\partial y^2}+\frac{b}{2}\Delta x\frac{\partial^2 u}{\partial x\,\partial y}\right]+\\ & O\left(\Delta x^2,\Delta x\Delta y,\Delta y^2\right),\end{aligned} \tag{3.31}$$

and the conditions for a second order N scheme are therefore:

$$C_T = 3\,,\quad C_R = -1\,,\text{ and } C_E = 2\,. \tag{3.32}$$

We finally arrive at the numerical approximation

$$\begin{aligned}-\vec{a}\cdot\vec{\nabla}u =& -a\frac{\partial u}{\partial x}-b\frac{\partial u}{\partial y}-\frac{a}{3}(\Delta x)^2\frac{\partial^3 u}{\partial x^3}-\frac{a}{2}\Delta x\Delta y\frac{\partial^3 u}{\partial x^2\,\partial y}-\frac{a}{2}(\Delta y)^2\frac{\partial^3 u}{\partial x\,\partial y^2}\\ & -\frac{b}{3}(\Delta y)^2\frac{\partial^3 u}{\partial y^3}+O\left(\Delta x^3,\Delta x^2\Delta y,\Delta x\Delta y^2,\Delta y^3\right).\end{aligned} \tag{3.33}$$

Note that node $u_{0,1}$ is a downstream node with respect to node $u_{0,0}$ given the advection speed $\vec{a}$. This is a somewhat unexpected development given the starting point of upwind schemes. It is due to the particular triangulation used in the derivation of the second order coefficients. On a grid consisting of equilateral triangles, the node is downstream. The first order N scheme for the linear advection equation on the grid of Fig. 3.8, (3.9), does not use node $u_{0,1}$. For the nonlinear equation, the RD N scheme uses node $u_{0,1}$ for the averaged advection speed. The FVD method uses the node $u_{0,1}$ for computing the edge flux between nodes $u_{0,1}$ and $u_{-1,0}$, and the advection speed. For the second order method, the contribution of node $u_{0,1}$ appears anyway in the FVD method due to the difference in weights : flux $f_{-1/2,1/2}$ is multiplied by C_T while flux $f_{0,1/2}$ is multiplied by C_E.

3.5.2. The second order N scheme in Finite Volume formulation for structured quadrilateral grids.

When substituting the coefficients of (3.32) in (3.28), and substituting the expressions for the edge fluxes, the second order N scheme can be written as

$$\begin{aligned} u_{0,0}^{n+1} = u_{0,0}^{n} &- \frac{a\Delta t}{\Delta x}\left[2u_{0,0} - 2u_{-1,0} - \tfrac{1}{2}u_{0,1} - \tfrac{1}{2}u_{-1,-1} + \tfrac{1}{2}u_{-2,-1} + \tfrac{1}{2}u_{-1,1}\right] \\ &- \frac{b\Delta t}{\Delta y}\left[\tfrac{3}{2}u_{-1,0} - \tfrac{3}{2}u_{-1,-1} - \tfrac{1}{2}u_{0,-1} + \tfrac{1}{2}u_{0,1} + \tfrac{1}{2}u_{-1,-2} - \tfrac{1}{2}u_{-1,1}\right] . \end{aligned} \tag{3.34}$$

The stencils for the derivatives u_x and u_y are given in Fig. 3.9.

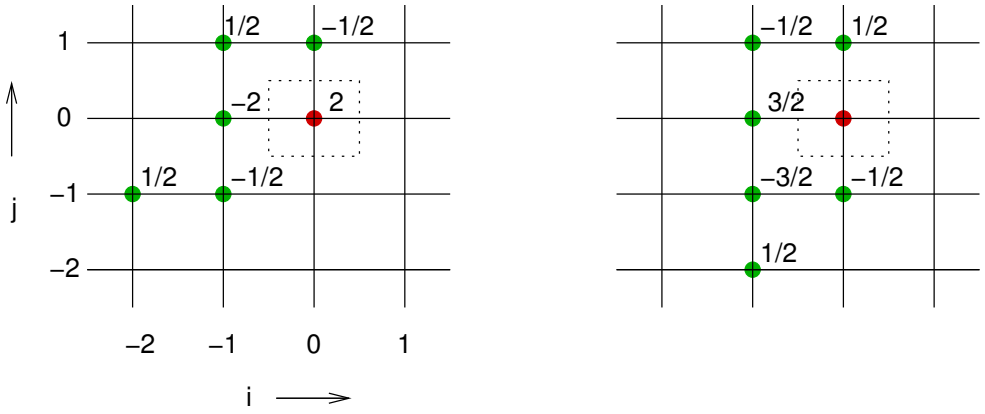

Figure 3.9. The stencils for $a\Delta y > b\Delta x > 0$ of the derivatives u_x and u_y of the second order N scheme of (3.34). Also indicated is the dual volume around $u_{0,0}$ in a FV formulation.

It is useful to separate the first order N scheme and the remaining terms, and write as differences :

$$\begin{aligned} u_{0,0}^{n+1} = u_{0,0}^{n} &- \frac{a\Delta t}{\Delta x}\left(u_{0,0} - u_{-1,0}\right) - \frac{b\Delta t}{\Delta y}\left(u_{-1,0} - u_{-1,-1}\right) \\ &- \frac{a\Delta t}{\Delta x}\left[(u_{0,0} - u_{-1,0}) - \tfrac{1}{2}(u_{0,1} - u_{-1,1}) - \tfrac{1}{2}(u_{-1,-1} - u_{-2,-1})\right] \\ &- \frac{b\Delta t}{\Delta y}\left[\tfrac{1}{2}(u_{0,1} - u_{0,0}) + \tfrac{1}{2}(u_{0,0} - u_{0,-1})\right. \\ &\qquad \left. - \tfrac{1}{2}(u_{-1,1} - u_{-1,0}) - \tfrac{1}{2}(u_{-1,-1} - u_{-1,-2})\right] . \end{aligned} \tag{3.35}$$

In order to write the update in terms of interface fluxes in a FV context, we use interface fluxes $f_{\pm 1/2,0}$ and $g_{0,\pm 1/2}$ for the volume around node $u_{0,0}$ as indicated in Fig. 3.9, where

the classical notation $f_{\pm 1/2,0}$ is now different from the previous section. Denote by $S_{i,j} = \Delta x\,\Delta y$ the cell volume around node (i,j), and by $R_{i,j}$ the cell residual. Similar to (2.2), the update for the structured FV scheme is

$$u_{i,j}^{n+1} - u_{i,j}^{n} = -\frac{\Delta t}{S_{i,j}}\, R_{i,j} = -\frac{\Delta t}{S_{i,j}}\, \left\{ (f_{i+1/2,j} - f_{i-1/2,j})\Delta y + (g_{i,j+1/2} - g_{i,j-1/2})\Delta x \right\} . \tag{3.36}$$

The interface fluxes can be easily obtained from (3.35),

$$\begin{aligned} f_{-1/2,0} &= a\left[u_{-1,0} + (u_{-1,0} - \tfrac{1}{2}u_{-1,1} - \tfrac{1}{2}u_{-2,-1})\right] \\ &= a\left[u_{-1,0} + (u_{-1,0} - u^*_{-3/2,0})\right] = a u_{-1/2,0}\,, \\ g_{0,-1/2} &= b\left[u_{-1,-1} + \tfrac{1}{2}\left(u_{0,0} + u_{0,-1} - u_{-1,0} - u_{-1,-2}\right)\right] \\ &= b\left[u_{-1,-1} + (u^*_{0,-1/2} - u^*_{-1,-1})\right] = b u_{0,-1/2}\,. \end{aligned} \tag{3.37}$$

The fluxes have been simplified introducing the averaged values $u^*_{-3/2,0} = {}^1\!/_2(u_{-1,1} + u_{-2,-1})$, $u^*_{-1,-1} = {}^1\!/_2(u_{-1,0} + u_{-1,-2})$, and $u^*_{0,-1/2} = {}^1\!/_2(u_{0,0} + u_{0,-1})$. In the following we will use the superscript * to indicate averaged values which can be thought to be located at nodal points or in between. Compared to the standard second order interface fluxes, $f_{-1/2,0} = a[u_{-1,0} + {}^1\!/_2(u_{-1,0} - u_{-2,0})]$ and $g_{0,-1/2} = b[u_{0,-1} + {}^1\!/_2(u_{0,-1} - u_{0,-2})]$, the difference is the use of eight instead of five points in the stencil, where most of the points of the stencil are used both in the x and in the y extrapolation. Moreover, the extrapolations are more compact in the sense that in the standard extrapolation the single extreme point of the extrapolation is both further in distance from the node used in the first order calculation, and further from the advection direction. The more directionally compact scheme reduces the cross-diffusion, like for the first order N scheme. For advection along the diagonal, $\vec{a} = {}^a\!/_h \begin{pmatrix} \Delta x \\ \Delta y \end{pmatrix}$, where $h^2 = \Delta x^2 + \Delta y^2$, the second order N scheme becomes $u_{0,0}^{n+1} - u_{0,0}^{n} = -{}^{a\Delta t}\!/_h \left(2u_{0,0}^n - {}^1\!/_2\{u_{-1,0}^n + u_{0,-1}^n\} - 2u_{-1,-1} + {}^1\!/_2\{u_{-2,-1}^n + u_{-1,-2}^n\}\right)$. This corresponds to the one-dimensional second order upwind scheme $u_0^{n+1} - u_0^n = -{}^{a\Delta t}\!/_{\Delta x}(2u_0^n - u_{-1/2}^n - 2u_{-1}^n + u_{-3/2}^n)$, and when we take $u_{-1/2} = {}^1\!/_2(u_0 + u_{-1})$ and $u_{-3/2} = {}^1\!/_2(u_{-1} + u_{-2})$, we get $u_0^{n+1} - u_0^n = -{}^{a\Delta t}\!/_{\Delta x}({}^3\!/_2 u_0^n - 2u_{-1}^n + {}^1\!/_2 u_{-2}^n)$. The one-dimensional discretization along the diagonal is therefore essentially the same as the one-dimensional discretization along a coordinate axis. Applying a one-dimensional solution for the case that the advection direction is along the x-axis or along the diagonal results in leaving the node $u_{0,0}$ unchanged. However, since the discretization involves nodal values off the diagonal in the case that the flow is along the diagonal, certain error terms remain when the transformation to a stream wise coordinate system is made. This scheme is further analyzed in [35], and it is shown that better discretizations can be found on structured grids.

3.5.3. The second order N scheme in Residual Distribution formulation.

The second order FVD N scheme can be rewritten as a RD scheme. The idea is to assemble the fluxes through the edges of a triangle in a residual, and to distribute the residual with the cell-averaged advection speed. It is important to use the proper advection speeds. The FVD N scheme uses two types of distribution coefficients: to edge nodes e_1 and e_2 according to (3.19) using the speed of the left triangle, and to the top node t_2 using the speed of the right triangle. For the coefficients of the second order N scheme, we can rewrite the coefficients of (3.32) as

$$C_T = 1 + F_L + F_R\,, \quad C_R = -F_R\,, \quad \text{and} \quad C_E = 1 + F_L\,. \tag{3.38}$$

Now we can separate the part of the flux which is distributed according to the right advection speed, from the part which depends on the left advection speed: the edge coefficients (C_E and the part F_L of C_T) depend on the left, the rest on the right triangle. In writing the second order RD N scheme, we again separate the treatment of the case of a triangle with inflow through one edge, or inflow through two edges. We arrive at the following distributions for the configurations depicted in Fig. 3.10:

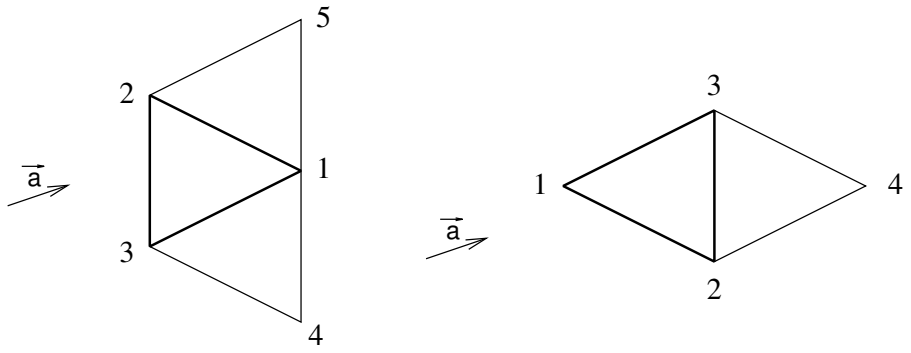

Figure 3.10. The second order RD scheme for triangle 123 in the case of one or two inflow sides.

$$\begin{aligned}
&\text{One inflow} && \text{Two inflow}\\
&\delta u_1 := \delta u_1 - 2\frac{\Delta t}{S_1} R_T\,, && \delta u_2 := \delta u_2 - 2\frac{\Delta t}{S_2}\left(\frac{a_2}{a_1} f_1 - f_2\right),\\
&\delta u_4 := \delta u_4 + \frac{\Delta t}{S_4}\left(\frac{a_2}{a_1} f_1 - f_2\right), && \delta u_3 := \delta u_3 - 2\frac{\Delta t}{S_3}\left(\frac{a_3}{a_1} f_1 - f_3\right),\\
&\delta u_5 := \delta u_5 + \frac{\Delta t}{S_5}\left(\frac{a_3}{a_1} f_1 - f_3\right), && \delta u_4 := \delta u_4 + \frac{\Delta t}{S_4} R_T\,.
\end{aligned} \tag{3.39}$$

When the RD is used with the conservative linearization of (3.7), the distribution reduces to

$$\begin{aligned}
&\text{One inflow} && \text{Two inflow}\\
&\delta u_1 := \delta u_1 - 2\frac{\Delta t}{S_1} R_T\,, && \delta u_2 := \delta u_2 - 2\frac{\Delta t}{S_2}\,\tfrac{1}{2} a_2 (u_2 - u_1)\,,\\
&\delta u_4 := \delta u_4 + \frac{\Delta t}{S_4}\,\tfrac{1}{2} a_2 (u_2 - u_1)\,, && \delta u_3 := \delta u_3 - 2\frac{\Delta t}{S_3}\,\tfrac{1}{2} a_3 (u_3 - u_1)\,,\\
&\delta u_5 := \delta u_5 + \frac{\Delta t}{S_5}\,\tfrac{1}{2} a_3 (u_3 - u_1)\,, && \delta u_4 := \delta u_4 + \frac{\Delta t}{S_4} R_T\,.
\end{aligned} \tag{3.40}$$

In the one-inflow case, twice the residual is sent to node 1, while the residual is subtracted from nodes 4 and 5 with the coefficients of the first order N scheme. For the two-inflow case, the nodes 2 and 3 now receive twice the update compared to the first order N scheme, while the residual is subtracted from the downstream node 4. In all the cases, the sum of the distributed updates adds up to the residual.

3.5.4. The directional central discretization.

The central scheme in one dimension can be interpreted as the average of two first order upwind schemes for advection speeds a and $-a$,

$$\frac{1}{2\Delta x}\left(f_{i+1} - f_{i-1}\right) = \frac{1}{2}\left\{\frac{1}{\Delta x}\left(f_{i+1} - f_i\right) + \frac{1}{\Delta x}\left(f_i - f_{i-1}\right)\right\}. \tag{3.41}$$

Applying this idea to two dimensions, we average the N scheme with advection speeds $\vec{a}$ and $-\vec{a}$. For the FVD formulation, this means averaging the distribution formulas of §3.2 for the two opposite advection directions. The distribution coefficients for the flux $f_e = {}^1\!/_2(u_{e_1} + u_{e_2})\vec{a}.\vec{n}_e$ are $\alpha^e_{e1} = {}^1\!/_2\vec{a}.(\vec{n}_{l1} + \vec{n}_{r1})$, $\alpha^e_{e2} = {}^1\!/_2\vec{a}.(\vec{n}_{l2} + \vec{n}_{r2})$, $\alpha^e_{t1} = {}^1\!/_2$, and $\alpha^e_{t2} = -{}^1\!/_2$. The sum of the distribution coefficients is zero since $\vec{n}_{l1} + \vec{n}_{r1} + \vec{n}_{l2} + \vec{n}_{r2} = 0$, see Fig. 3.5.

The interface fluxes used in (3.36) on a structured grid for $a\Delta y > b\Delta x > 0$ are

$$f_{i+1/2,j} = \tfrac{1}{2}\left(f_{i+1,j} + f_{i,j}\right) , \quad g_{i,j+1/2} = \tfrac{1}{2}\left(g_{i+1,j+1} + g_{i-1,j}\right) . \tag{3.42}$$

The directional central scheme is then

$$u^{n+1}_{i,j} - u^n_{i,j} = -\frac{\Delta t}{S_{i,j}}\left\{\tfrac{1}{2}(f_{i+1,j} - f_{i-1,j})\Delta y + \tfrac{1}{2}(g_{i+1,j+1} - g_{i+1,j} - g_{i-1,j} + g_{i-1,j-1})\Delta x\right\} . \tag{3.43}$$

The stencil is as expected the combination of the N scheme with its opposite, which as required eliminates the central node. The stencils for the derivatives u_x and u_y are shown in Fig. 3.11.

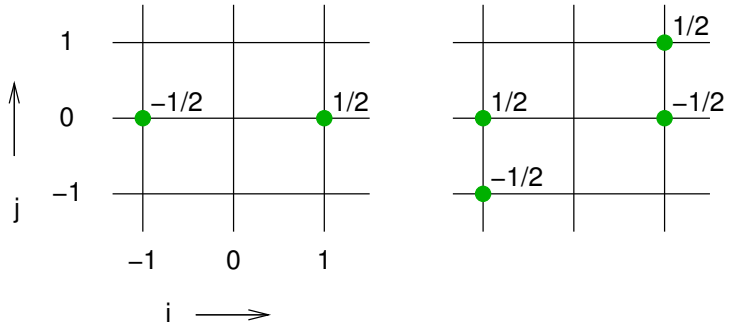

Figure 3.11. The stencils for the derivatives u_x and u_y of the second order directional central scheme for $a\Delta y > b\Delta x > 0$ of (3.43).

For advection along the diagonal, the scheme for the linear advection equation reduces to the one-dimensional central scheme along the streamline, which is $u^{n+1}_{0,0} - u^n_{0,0} = -{}^{a\Delta t}\!/_h\,(u_{1,1} - u_{-1,-1})$. The directional central scheme shares the increased accuracy with the N scheme. This is further elaborated in [35].

The RD formulation uses the average of the updates of (3.4) and (3.16).

3.5.5. Other directional schemes.

The methodology used so far can be used to derive other directional schemes starting from the N scheme, e.g. a fourth order central scheme, which is given by

$$\begin{aligned} 12\Delta x u_x &= u_{-1,1} - 3u_{0,1} + 3u_{1,1} - u_{2,1} - 6u_{-1,0} + 6u_{1,0} \\ &\quad + u_{-2,-2} - 3u_{-1,-1} + 3u_{0,-1} - u_{1,-1} , \\ 12\Delta y u_y &= u_{-1,-2} - 3u_{-1,-1} + 3u_{-1,0} - u_{-1,1} - 6u_{0,-1} + 6u_{0,1} \\ &\quad + u_{1,-1} - 3u_{1,0} + 3u_{1,1} - u_{1,2} . \end{aligned} \tag{3.44}$$

The stencils are given in Fig. 3.12.

It is a central discretization with directional improved behavior with respect to the standard one-dimensional approximations. Like the second order N scheme, other, and in some respects better discretizations can be derived [35].

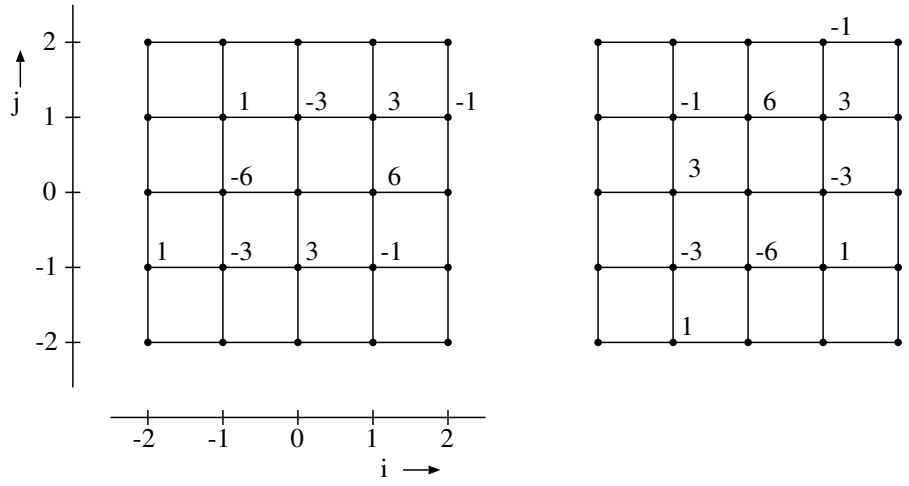

Figure 3.12. The stencils of u_x and u_y for the directional central approximations (3.44).

The first residual distribution scheme was the Lax-Wendroff scheme described by Ni on quadrilaterals [18]. However, like all versions of the Lax-Wendroff scheme since, it incorporates a one-dimensional grid-aligned central scheme, which is less optimal than the directional central scheme of the previous section.

Other first order schemes can be used in the distribution to nodes further away, such as the LDA scheme [26]. Since the LDA scheme can be written as the N scheme plus a correction term, this means distributing the correction term.

In the derivation of (3.31), we apply the consistency condition in order to obtain an approximation for the gradient. We can of course apply the consistency condition for a second derivative, ∇^2, or any other derivative using wider distribution stencils. This approach is used in [35].

The FVD method can also be used with the quadrilateral elements used by Paillère et al. [71].

4. Three-dimensional Flux Vector Distribution schemes.

We will look at discretizations derived from the N scheme on structured tetrahedral grids in three dimensions. In [35], discretizations other than the N scheme are discussed on structured and unstructured grids in N dimensions.

4.1. Directional discretizations in three dimensions on tetrahedra.

In three dimensions, no grid exists which consists of regular tetrahedra with equilateral surfaces. There are two well-known regular structures in three dimensions, the icosahedron and the diamond structure. The first has a regular surface consisting of equilateral triangles, but the distance from one of the constituting vertices to the central node is about 5% shorter than the length of the equilateral triangle. The central node is surrounded by twelve vertices and twenty triangles meet at the central vertex. The second is a collection of carbon atoms in a regular tetrahedral structure. This does not bring us any further since the carbon atoms form a face centered cubic cell [72], which cannot be used in our context.

The discretizations on an icosahedron is discussed in [35]. Here, we consider a hexahe-

dron, dissected in either five or six tetrahedra. The nodes of the tetrahedra are the nodes of the hexahedron.

The splitting in five tetrahedra is possible in two different ways, one of which is shown in Fig. 4.1. This dissection of the hexahedron is without the use of a body diagonal. The surface diagonals on opposite sides of the hexahedron have different orientation, and both types of dissections are needed to fill the space.

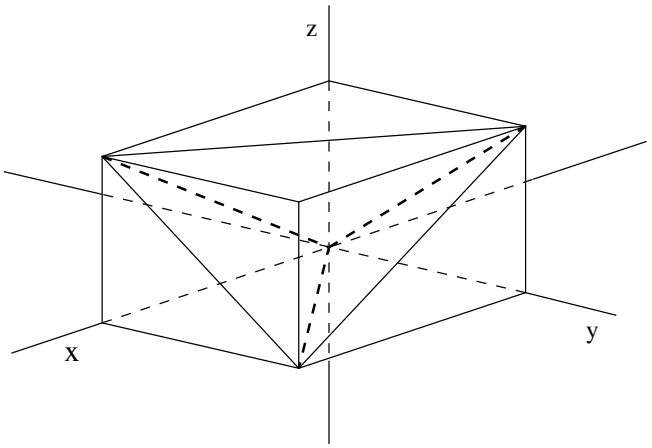

Figure 4.1. Dissection of a hexahedron in five tetrahedra, one of two possibilities.

The first order N scheme, expressed in a distribution formulation such as (3.18) then results in an inconsistent discretization, and does not result in the N scheme on the underlying structured grid. The expression for the update is too cumbersome to include here, but it can be easily seen that the node (-1,-1,-1) is absent from the approximation of the first derivative at (0,0,0). The central directional discretization which is the average of two opposite N-discretizations as described in §3.5.4 is therefore also inconsistent.

The same happens with the dissection in six tetrahedra. There are eight dissections which have the same direction of the side diagonals on opposite walls of the hexahedron. One example is shown in Fig. 4.2.

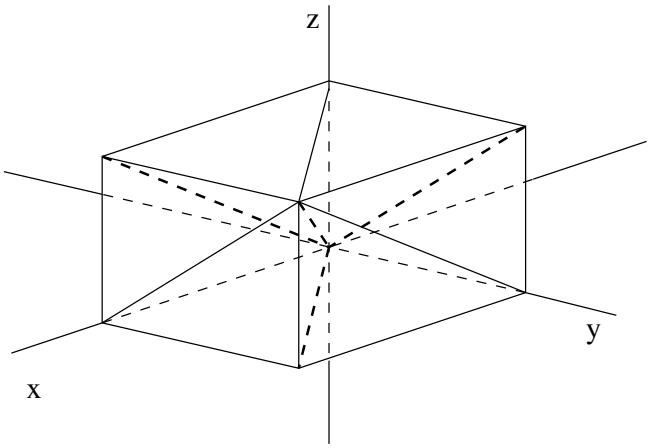

Figure 4.2. Dissection of a hexahedron in six tetrahedra, one of the eight possibilities which has the side diagonals parallel.

The distribution according to (3.18) gives inconsistent discretizations, and does not

revert to the structured N scheme. It does not only depend on the unknowns at (0,0,0), (-1,0,0), (-1,-1,0), and (-1,-1,-1), but also on the variables at (0,-1,0), (-1,0,-1), and (0,0,1). The central directional discretization is again inconsistent.

The problem of inconsistencies seems unavoidable in three dimensions for directional discretizations on structured tetrahedral grids based on the N scheme. Remark that the residual on a cube can be written as a sum of differences over the four body diagonals, and therefore defies to be cast in a form based on the N scheme.

In two dimensions, a regular triangulation exists, and inconsistencies appear only on irregular grids. In three dimensions, the absence of a regular tetrahedral grid leads to inconsistent directional discretizations. It would be interesting to see which impact the inconsistencies have on the numerical solution. Most likely, the average advection speed will be found back over a number of cells. Current unstructured solvers do not seem to exhibit a dominant deviation of the advection direction. However, the reduction in accuracy may hurt, especially for higher order approximations.

5. Conclusion.

In this paper we have considered numerical schemes for systems of hyperbolic equations from the point of view of distributing the fluxes. This idea is a logic consequence of the distribution schemes for residuals which have been under development for some thirty years now. The shift of viewpoint has been advantageous, and the main results of this paper are the following :

The Flux Vector Distribution formulation. The FVD method is a convenient way of formulating space discretizations. The commonly available schemes are readily recovered, while the formulation of new discretizations is easy. Distribution is based on directional coefficients, which can also be used in the RD formulation.

Flux splitting is common to FVS and FDS. It is known that some FVS and FDS have a flux splitting in common. The most basic flux splitting is the decomposition in an entropy part and into acoustic parts. The separate treatment of the entropy in two and three dimensions may be advantageous. As FVS this is known as the Steger-Warming splitting, while when used with the conservative linearization it is known as Roe's FDS. This flux splitting also appears when the matrix extension is made of the scalar schemes. When using the extension to systems of the flux of Engquist and Osher, the integration path which keeps the Mach number constant again gives the entropy-acoustic splitting. Other integration paths are possible, using the Riemann invariants as in the FDS of Osher.

Higher order directional schemes. In two space dimensions, directional central and upwind schemes can be easily derived for any order. This is generally based on a Taylor series development, such as fully exploited in [35], but in this paper we have focused on distribution coefficients which are derived from the N scheme. The second order directional upwind scheme is different from all previous attempts for directionally higher order upwind schemes. Perhaps the most surprising result is the second order directional central scheme. The directional central scheme is a building block for, among others, the Lax-Wendroff type schemes. In fact, the directional ideas can be applied to any discretization for advection phenomena, including compact schemes.

Inconsistent schemes. At several occasions we encountered inconsistent space discretizations. To begin with, higher order schemes using limiters are locally inconsistent. Central schemes with a TVD artificial viscosity have the same problem. The inconsistency

is in the advection speed. While the schemes are shown to be inconsistent, the effects have so far gone unnoticed. The N scheme on triangles is locally inconsistent on an irregular triangulation. In three dimensions, asymmetric discretizations are inconsistent on regular tetrahedral meshes.

References

[1] S.K. Godunov. A finite-difference method for the numerical computation of discontinuous solutions of the equations of fluid dynamics. *Mat. Sbornik*, 47:357–393, 1959. Citation on p. 1.

[2] A. Harten, P.D. Lax, and B. van Leer. On upstream differencing and Godunov-type schemes for hyperbolic conservation laws. *SIAM Review.*, 25:35–61, January 1983. Citations on p. 1, 3, and 8.

[3] B. van Leer. On the relation between the upwind-differencing schemes of Godunov, Engquist-Osher and Roe. *SIAM J. Num. Anal.*, 5(1), mar 1984. Citations on p. 1, 3, and 8.

[4] B. van Leer. Towards the ultimate conservative difference scheme. II. Monotonicity and conservation combined in a second-order scheme. *J. Comp. Phys.*, 14:361–370, 1974. Citations on p. 1 and 12.

[5] P. K. Sweby. High resolution schemes using flux limiters for hyperbolic conservation laws. *SIAM J. Num. Anal.*, 21(5):995–1011, 1984. Citations on p. 1 and 12.

[6] B. van Leer, J.L. Thomas, P.L. Roe, and R.W. Newsome. A comparison of numerical flux formulas for the Euler and Navier-Stokes equations. *AIAA*, (87-1104-CP), 1987. Citation on p. 1.

[7] B. van Leer. Flux-vector splitting for the Euler equations. In *Proc. 8^{th} Int. Conf. on Num. Meth. in Fl. Dyn.*, number 170 in Lecture Notes in Physics, pages 507–512. Springer, Berlin, 1982. Citation on p. 1.

[8] D.S. Butler. The numerical solution of hyperbolic systems of partial differential equations in three independent variables. In *Proceedings of the Royal Society of London*, volume 255A, pages 232–252, 1960. Citation on p. 1.

[9] G.D. Raithby. Skew upstream differencing schemes for problems involving fluid flow. *Comput. Meth. Appl. Mech. Eng.*, 9:153–164, 1976. Citation on p. 1.

[10] S.F. Davis. A rotationally biased upwind difference scheme for the Euler equations. *J. Comp. Phys.*, 56:65–92, 1984. Citation on p. 1.

[11] J.G. Rice and R.J. Schnipke. A monotone streamline upwind finite element method for convection-dominated flows. *Comp. Meth. in Appl. Mech. and Eng.*, 48:313–327, 1985. Citation on p. 1.

[12] T.J.R. Hughes, M. Mallet, and A. Mizukami. A new finite-element formulation for computational fluid dynamics, II. Beyond SUPG. *Comp. Meth. Appl. Mech. & Eng.*, 84, 1986. Citation on p. 1.

[13] H. Deconinck, C Hirsch, and J. Peuteman. Characteristic decomposition methods for the multidimensional Euler equations. In F.G. Zhuang and Y.L. Zhu, editors, *Lecture Notes in Physics*, number 264, pages 216–221. Springer, Berlin, 1986. Citation on p. 1.

[14] B. Koren. Low-diffusion rotated upwind schemes, multigrid and defect correction for steady, multi-dimensional Euler flows. In *International Series of Numerical Mathematics*, volume 98. Birkhäuser Verlag, Basel, 1991. Citations on p. 1 and 17.

[15] D.W. Levy, K.G. Powell, and B. van Leer. An implementation of a grid-independent upwind scheme for the Euler equations. *AIAA*, (89-1931-CP), June 13-15 1989. Buffalo, New York, USA. Citation on p. 1.

[16] C. Hirsch and C. Lacor. Upwind algorithms based on a diagonalization of the multidimensional Euler equations. *AIAA*, (89-1958-CP), 1989. Citation on p. 1.

[17] B. van Leer. Progress in multidimensional upwind differencing. Technical Report 92-43, ICASE, NASA Langley Research Center, Hampton, Virginia, sep 1992. Citation on p. 1.

[18] R.H. Ni. A multiple-grid scheme for solving the Euler equations. *AIAA J.*, 20:1565–1571, 1982. Citations on p. 1, 4, 9, and 29.

[19] H.G. Hall. Cell-vertex multigrid schemes for the solution of the Euler equations. In K.W. Morton and M.J. Baines, editors, *Numerical Methods for Fluid Dynamics II*, pages 303–365. Clarendon, Oxford, 1986. Citations on p. 1 and 4.

[20] K.W. Morton, P.N Childs, and M. A. Rudgyard. Technical Report NA88/5, Oxford University Computing Laboratory, 1988. Citation on p. 1.

[21] P.L. Roe. Fluctuations and signals, a framework for numerical evolution problems. In K.W. Morton and M.J. Baines, editors, *Numerical Methods for Fluid Dynamics I*, pages 219–257. Academic Press, 1982. Citations on p. 1, 2, 4, 9, and 15.

[22] P.L. Roe. Linear advection schemes on triangular meshes. CoA Report 8720, Cranfield Institute of Technology, Cranfield, Bedford, nov 1987. Citations on p. 1, 4, 9, 13, 15, 16, and 20.

[23] H. Deconinck, R. Struijs, and P.L. Roe. Fluctuation splitting for multidimensional convection problems : an alternative to finite volume and finite element methods. In *Von Karman Institute Lecture Series 1990-03*, Computational Fluid Dynamics. Von Karman Institute, Brussels, March 5-9 1990. Citation on p. 1.

[24] R. Struijs. The fluctuation splitting method. In C.B. Vreugdenhil and B. Koren, editors, *Notes on Numerical Fluid Mechanics*, volume 45, chapter 11, pages 261–289. Vieweg, Braunschweig, 1993. Numerical Methods for Advection-Diffusion Problems. Citation on p. 1.

[25] H. Paillère, H. Deconinck, R. Struijs, L.M. Mesaros P.L. Roe, and J.-D. Müller. Computations of inviscid compressible flows using fluctuation-splitting on triangular meshes. *AIAA*, (93-3301-CP), 1993. Citation on p. 1.

[26] R. Struijs, H. Deconinck, P. de Palma, P. Roe, and K.G. Powell. Progress on multidimensional upwind Euler solvers for unstructured grids. *AIAA*, (91-1550), 1991. Citations on p. 2, 16, 22, and 29.

[27] P. De Palma, H. Deconinck, and R. Struijs. Investigation of Roe's 2D wave decomposition models for the Euler equations. Technical Report 172, Von Karman Institute, Brussels, jul 1990. Citation on p. 2.

[28] H. Paillère. *Multidimensional upwind residual distribution schemes for the Euler and Navier-Stokes equations on unstructured grids.* PhD thesis, Université Libre de Bruxelles, 1995. Citation on p. 2.

[29] K.W. Morton and S.M. Stringer. Finite volume methods for inviscid and viscous flows, steady and unstead. In *Von Karman Institute Lecture Series 1995-02*, Computational Fluid Dynamics. Von Karman Institute, Brussels, mar 13-17 1995. Citation on p. 2.

[30] E. van der Weide and H. Deconinck. Positive matrix distribution schemes for hyperbolic systems, with application to the Euler equations. In *ECCOMAS 96*. John Wiley & Sons, 1996. Citations on p. 2 and 22.

[31] R. Abgrall. Toward the ultimate conservative scheme : following the quest. *J. Comp. Physics*, 167(1):277–315, 2001. Citations on p. 2 and 22.

[32] A. Lerat and C. Corre. A residual-based compact scheme for the compressible Navier-Stokes equations. *J. Comp. Physics*, 170:642–675, 2001. Citation on p. 2.

[33] R. Abgrall and M. Mezine. Construction of second order accurate monotone and stable residual distribution schemes for unsteady flow problems. *J. Comp. Physics*, 188(1):16–55, 2001. Citation on p. 2.

[34] R. Abgrall and P. L. Roe. Higher order fluctuation schemes on triangular meshes. *J. Sci. Comp.*, 19(1-3):3–36, dec 2003. Citation on p. 2.

[35] R. Struijs. A basis for discretizations. Available at `http://www.ma.utexas.edu/mp_arc`, January 2010. Citations on p. 2, 15, 17, 26, 28, 29, and 31.

[36] E.M. Murman and J.D. Cole. Calculation of plane steady transonic flows. *AIAA-J*, 9(1):114–121, 1971. Citation on p. 6.

[37] B. Engquist and S. Osher. Stable and entropy satisfying approximations for transonic flow calculations. *Math. Comp.*, 34(149):45–75, 1980. Citations on p. 6 and 8.

[38] L.C. Huang. Pseudo-unsteady difference schemes for discontinuous solutions of steady-state one-dimensional fluid dynamic problems. *J. Comp. Physics*, 42:195–211, 1981. Citations on p. 8 and 20.

[39] R. Courant, E. Isaacson, and M. Reeves. On the solution of nonlinear hyperbolic differential equations by finite differences. *Comm. Pure and Applied Mathematics*, 5:243–255, 1952. Citation on p. 8.

[40] F. Coquel and M.-S. Liou. Hybrid upwind splitting (HUS) by a field by field decomposition. Technical Report TM 106843, NASA, 1995. Citation on p. 8.

[41] B. van Leer, W.-T. Lee, and K.G. Powell. Sonic point capturing. *AIAA*, (89-1945-CP), 1989. Citation on p. 9.

[42] M. Rudgyard. Upwind iteration methods for the cell vertex scheme - one dimensional problems. Technical Report 90/5, Oxford University Computing Laboratory, Numerical Analysis Group, 1990. Citation on p. 9.

[43] P. Crumpton, J.A. Mackenzie, and K.W. Morton. Cell vertex algorithms for the compressible Navier-Stokes equations. *J. Comp. Phys.*, 109:1–15, 1993. Citation on p. 9.

[44] P.L. Roe. Approximate riemann solvers, parameter vectors and difference schemes. *J. Comp. Phys.*, 43:357–372, 1981. Citations on p. 9 and 12.

[45] D. Sidilkover. *Numerical solution to steady-state problems with discontinuities.* PhD thesis, The Weizmann Institute of Science, Rehovot, Israel, 1989. Citations on p. 9, 10, and 17.

[46] P.L. Roe. Upwind differencing schemes for hyperbolic conservation laws with source terms. In Cassano, Raviart, and Serre, editors, *Proc. Conf. hyperbolic problems*, pages 41–51. Springer, 1986. Citation on p. 9.

[47] B. Koren. A robust upwind discretization method for advection, diffusion and source terms. In C.B. Vreugdenhil and B. Koren, editors, *Numerical methods for advection diffusion problems*, volume 45, chapter 5. Vieweg, Braunschweig, 1993. Citation on p. 9.

[48] R.J. Leveque. Balancing source terms and flux gradients in high-resolution godunov methods ; the quasi steady wave-propagation algorithm. *J. Comp. Phys.*, 146:346–365, 1998. Citation on p. 9.

[49] S. Osher. Numerical solution of singular perturbation problems and hyperbolic systems of conservation laws. In O. Axelsson, editor, *Mathematical Studies*, number 47. Amsterdam :North Holland, 1981. Citation on p. 11.

[50] S. Osher and F. Solomon. Upwind difference schemes for hyperbolic systems of conservation laws. *Mathematics of Computation*, 38(158):339–374, April 1982. Citation on p. 11.

[51] P.W. Hemker and S.P. Spekreijse. Multiple grid and osher's scheme for the efficient solution of the steady Euler equations. *Applied Numerical Mathematics*, 2:475–493, 1986. Citation on p. 11.

[52] J.L. Steger and R.F. Warming. Flux vector splitting of the inviscid gasdynamic equatons with application to finite difference methods. *J. Comp. Physics*, 40(2):263–293, April 1981. Citation on p. 11.

[53] S.R. Chakravarthy, D.A. Anderson, and M.D. Salas. The split coefficient matrix method for hyperbolic systems of gas dynamic equations. *AIAA*, (80-0268-CP), 1980. Citation on p. 12.

[54] A. Harten. High-resolution schemes for hyerbolic conservation laws. *J. Comp. Phys.*, 49:357–393, 1983. Citation on p. 12.

[55] B. van Leer. Towards the ultimate conservative difference scheme. IV. A new approach to numerical convection. *J. Comp. Phys.*, 23:276–299, 1977. Citation on p. 12.

[56] B. van Leer. Towards the ultimate conservative difference scheme. V. A second-order sequel to Godunov's method. *J. Comp. Phys.*, 32:101–136, 1979. Citation on p. 12.

[57] J.P. Boris and D.L. Book. Flux-corrected transport. I. SHASTA, a fluid transport algorithm that works. *J. Comp. Phys.*, 11:38–69, 1973. Citation on p. 12.

[58] W.K. Anderson, J.L. Thomas, and B. van Leer. Comparison of finite volume flux vector splittings for the Euler equations. *AIAA-J*, 24(1453-60), 1986. Citation on p. 12.

[59] S.P. Spekreijse. *Multigrid solution of the steady Euler equations.* PhD thesis, Delft, The Netherlands, 1987. Citation on p. 12.

[60] C. Hirsch. *Numerical computation of internal and external flow.* Vol. 2, Computational methods for inviscid and viscous flows. J. Wiley & Sons, New York, 1990. Citation on p. 12.

[61] K.G. Powell, B. van Leer, and P.L. Roe. Multi-dimensional cell-vertex schemes for convection. Technical report, University of Michigan, Ann Arbor, may 1990. Citation on p. 13.

[62] R. Struijs. *A multidimensional upwind discretization method for the Euler equations on unstructured grids.* PhD thesis, University of Delft, the Netherlands, 1994. Citations on p. 13 and 22.

[63] G. Bourgois, H. Deconinck, P.L. Roe, and R. Struijs. Multi-dimensional upwind schemes for scalar advection on tetrahedral meshes. In Ch. Hirsch, J. Périaux, and W. Kordulla, editors, *First Eur. Comp. Fluid Dyn. Conf., Sept. 7-11,1992*. Elsevier, Amsterdam. Citation on p. 16.

[64] P.L. Roe and D. Sidilkover. Optimum positive linear schemes for advection in two and three dimensions. *SIAM J. Num. Anal.*, 29(6):1505–1825, 1992. Citation on p. 17.

[65] C. Hirsch. Compact schemes for two-dimensional convection problems. In *Von Karman Institute Lecture Series 1991-04*, Computational Fluid Dynamics. Von Karman Institute, Brussels, February 18-22 1991. Citation on p. 17.

[66] P.L. Roe. A conservative linearization of the multidimensional Euler equations. CoA Report 8910, Cranfield Institute of Technology, Cranfield, Bedford, 1989. Citation on p. 22.

[67] C.K. Lombard, J. Oliger, and J.Y. Yang. A natural conservative flux difference splitting for the hyperbolic systems of gas dynamics. *AIAA*, (82-0976-CP), 1982. Citation on p. 22.

[68] E. Dick. A multigrid flux-difference splitting method for steady Euler equations. In S.F. McCormick, editor, *Proc. 3^d Copper Mountain Conference*, volume 110 of *Lecture Notes in Pure and Applied Mathematics*, apr 1989. Citation on p. 22.

[69] M. Rudgyard. private communication, 1993. Citation on p. 22.

[70] For information see `http://www.sciface.com`. Citation on p. 24.

[71] H. Paillère, E. van der Weide, and H. Deconinck. Multidimensional upwind methods for inviscid and viscous flows. In *Von Karman Institute Lecture Series 1995-02*, Computational Fluid Dynamics. Von Karman Institute, Brussels, March 1995. Citation on p. 29.

[72] C. Kittel. *Introduction to solid state physics.* John Wiley & Sons, New York, 1968. Citation on p. 29.